Establishment of microglial precursors derived from human induced pluripotent stem cells to model SOD1-mediated amyotrophic lateral sclerosis

PhD thesis

In fulfillment of the requirements for the degree
“Doctor rerum naturalium”
at the
Faculty of Mathematics and Natural Sciences
of the
Rheinische-Friedrich-Wilhelms University of Bonn

Submitted by
Kristin Roy
born in
Leipzig, Germany

Bonn, August 2012

Angefertigt mit Genehmigung der Mathematisch Naturwissenschaftlichen Fakultät der Rheinischen Friedrich-Wilhelms Universität Bonn.

1. Gutachter: Prof. Dr. Harald Neumann
2. Gutachter: Prof. Dr. Joachim Schultze

Tag der Promotion: 24.01.2013
Erscheinungsjahr: 2013

I Table of Content

II Abbreviations

Aβ	amyloid beta
ALS	amyotrophic lateral sclerosis
ANOVA	analysis of variance
ATP	adenosintriphosphat
BSA	bovine serum albumine
CCS	copper chaperone for SOD1
CD	cluster of differentiation
CNS	central nervous system
CO_2	carbon dioxide
CX3CL1	CX3 chemokine ligand 1
CX3CR1	CX3 chemokine receptor 1
DAPI	4',6-diamidino-2-phenylindole
DHE	dihydroethidium
DMEM	Dulbecco’s Modified Eagle's Medium
DMSO	dimethylsulfoxide
DNA	deoxyribonucleic acid
dNTP	deoxynucleotide triphosphate
E	embryonic day
EB	embryoid bodies
EDTA	ethylenediaminetetraacetic acid
ESC	embryonic stem cell
ESdM	mouse embryonic stem cell derived microglia
ETC	electron transport chain
FACS	fluorescence activated cell sorting
FCS	fetal calf serum
FGF	fibroblast growth factor
Fig.	figure
Fn	fibronectin
g	gram
GAPDH	glyceraldehyde-3-phosphate dehydrogenase
GFAP	glial fibrillar acidic protein
GFP	green fluorescent protein

GM-CSF	granulocyte macrophage colony stimulating factor
GTP	guanosintriphosphat
H_2O	water
h	hour
HCl	hydrochloride acid
hESC	human embryonic stem cells
H_2O_2	hydrogen peroxide
HEK	human embryonic kidney
HEPES	(4-(2-hydroxyethyl)-1-piperazineethanesulfonic acid
HRP	horse radish peroxidase
Iba1	ionized calcium binding adaptor molecule
IL	interleukin
IFNγ	interferon γ
iNOS	inducible nitric oxide synthetase
iPS	induced pluripotent stem cell
iPSdM	induced pluripotent stem cell derived microglial precursors
Klf4	Krüppel like factor 4
KO/SR	knockout serum replacement
LPS	lipopolysaccharide
M	molar
MEF	murine embryonic fibroblasts
mg	milligram
MHC	major histocompatibility complex
min	minute
ml	milliliter
mM	millimolar
mSOD1	mutant superoxide dismutase 1
MTT	(3-(4,5-dimethylthiazol-2-yl)-2,5-dipenyl tetrasodium bromide)
NADH	Nicotinamide adenine dinucleotide
NADPH	Nicotinamide adenine dinucleotide phosphate
NEAA	non essential amino acids
ng	nanogram
nm	nanometer
NO	nitric oxide

Oct-4	octamer 4
PAGE	poly-acrylamid gel electrophoresis
PBS	phosphate buffered saline
PCR	polymerase chain reaction
PE	phycoerythrin
Pen/Strep	penicillin/ streptomycin
PFA	paraformaldehyde
PGK	phosphoglycerate kinase
PLL	poly-L-lysin
PLO	poly-L-ornithin
PLP	proteolipid protein
PtdSer	phosphatidylserine
rh	recombinant human
RNA	ribonucleic acid
rpm	rounds per minute
ROS	reactive oxygen species
RT	room temperature
RT-PCR	reverse transcription- polymerase chain reaction
s	second
SCID	severe combined immunodeficiency
SDS	sodium dodecyl sulfate
SEM	standard error of the mean
Siglec	sialic binding immunoglobulin-like lectin
SOD1	superoxide dismutase 1
Sox2	SRY box-containing gene 2
SSEA	stage-specific embryonic antigen
TGFβ	transforming growth factor β
TLR	toll like receptor
TNFα	tumor necrosis factor alpha
Tris	tris(hydroxymethyl)-aminomethane
U	unit
UTP	uridintriphosphat
wt	wildtype
µm	micrometer

III Abstract

Microglia, the resident immune cells of the central nervous system (CNS), are responsible for tissue homeostasis and host defense. After activation, they can also be involved in a wide range of neurodegenerative diseases including amyotrophic lateral sclerosis (ALS). In ~10 % of the hereditary ALS cases, the disease is caused by a mutation in the superoxide dismutase 1 (SOD1) gene. The exact pathophysiological role of mutant SOD1 in human microglia is still unclear.

Microglial precursors were generated from human induced pluripotent stem (iPS) cells to a proliferating cell line to overcome the limitations of primary microglia. The obtained iPS-derived microglial precursor (iPSdM) cells were positively stained for Iba1 and CD68, markers widely expressed on microglia. Moreover, flow cytometry analysis demonstrated the expression of typical microglial markers like CD11b, CD45, CD49d, CD86, CD206 and CX3CR1 whereas the cells were negative for the hematopoietic stem cell marker CD34. Functional analysis revealed the capability of beads and fibrillary amyloid β phagocytosis. Furthermore, iPSdM showed upregulation of tumor necrosis factor α (TNFα) gene transcription after lipopolysaccharide (LPS) stimulation and chemokine-directed migration towards CX3CL1. Transplantation of iPSdM into the hippocampus of immunodeficient mice showed the capability of these cells to migrate and integrate into the brain parenchyma.

Next, iPSdM were genetically engineered to express distinct human mutant SOD1 to model SOD1-mediated ALS. Mutant SOD1 expressing iPSdM showed no differences in cytokine production or alterations in mitochondrial enzymes in comparison to SOD1 wildtype expressing cells. In contrast, iPSdM expressing SOD1-G37R or SOD1-G93A showed increased induced superoxide production after stimulation with TNFα, LPS or interferon γ, respectively.

Thus, data demonstrate the generation of human microglial precursor cell lines from iPS cells and their application as neuroinflammatory disease model for mutant SOD1-mediated ALS.

1 Introduction

1.1 Microglia

1.1.1 Microglia in the CNS

The central nervous system (CNS) consists of two main cell types: neurons and glial cells. Neurons build a network throughout the nervous system and transmit information through electrical conduction. Glial cells play a supportive and protective role to neurons and are not directly involved in the conduction process. Glial cells can be subdivided into two main classes: macroglia consisting of astrocytes and oligodendrocytes and microglia.

Microglia are the resident immune cells of the CNS and constitute about 10 % of all brain cells (Ransohoff and Perry, 2009). Ramon Y Cajal defined them as the third group of CNS cells termed *mesoglia* (Rezaie and Male, 2002). Del Rio-Hortega was the first defining the term *microglia* and proposed that they can change their morphology dependent on the activation stage (del Rio-Hortega, 1933). Microglia are distributed throughout the whole brain parenchyma but are predominant in the grey matter with highest concentration in the hippocampus, substantia nigra, olfactory telencephalon and basal ganglia (Block *et al*., 2007). Microglia are mainly involved in tissue homeostasis by scavenging invading microorganisms and apoptotic cells and furthermore act as immune effector cells (Kettenmann *et al.*, 2011).

1.1.2 Origin of Microglia

Nowadays it is suggested that microglia populate the brain in two waves. In mice, microglia first colonize the brain during embryonic development around embryonic day (E) 8.5-10 in the neuroepithelium (Alliot *et al.*, 1999). The second wave occurs in the brain during fetal development from E13.5 until birth (Chan *et al.*, 2007). Some authors suggested the yolk sac as the tissue of origin (Alliot *et al.*, 1999, Kaur *et al.*, 2001). Alliot and colleagues (1999) reported that cells with properties of microglial precursors can be first detected at embryonic day E8 in mice and that most of these progenitors originate from the yolk sac. A recent publication clearly showed that microglial cells develop in the yolk sac from immature macrophages before day E8 (Ginhaux *et al.*, 2010). These cells migrate into the CNS before

primitive or definite hematopoiesis occurs. Experiments demonstrated that microglia develop independently from cells arising in the bone marrow and peripheral myeloid cells do not contribute to maintenance of adult microglia (Ginhaux *et al.*, 2010; Saijo and Glass, 2011).

1.1.3 Functions of microglia

In the healthy CNS, microglia are often termed as resting cells displaying a ramified morphology (Fig. 1.1) characterized by a small round cell body, extensively ramified processes and low expression of surface antigens (Garden and Möller, 2006). Processes of microglia directly contact astrocytes and neuronal cell bodies and continuously scan their environment. Time-lapse imaging using *in vivo* two-photon microscopy revealed that the somata of microglial cells remained fixed whereas the processes were remarkably motile undergoing withdrawal and new formation (Nimmerjahn *et al.*, 2005). Resting microglia release immuno-suppressant factors such as interleukin (IL)-10 and transforming growth factor β (TGFβ) as well as neurotrophic factors crucial for neuronal survival (Hanisch, 2002; Ransohoff and Perry, 2009). Interaction of microglia with neurons seems to be important to keep them in a resting stage. In the healthy CNS, neurons suppress microglial activation through cell-cell contacts and secreted factors. For example, microglia are the only cell type expressing CX3 chemokine receptor 1 (CX3CR1) in the CNS. Secretion of the ligand CX3 chemokine ligand 1 (CX3CL1) by neurons restrains microglial activation whereas interruption of this signaling resulted in increased neuronal death (Biber *et al.*, 2007).

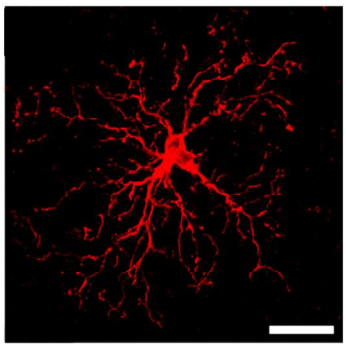

Fig.1.1: Microglial cell in the mouse CNS. Highly ramified microglia stained with an antibody directed against ionized calcium binding adaptor molecule (Iba1). Scale bar: 20 µm. Modified from Soulet and Rivest, 2008.

In response to immunological stimuli or brain injuries, ramified microglia transform into activated cells (Fig. 1.2). Activation leads to an immediate microglial response resulting in migration to the lesion site, phagocytosis of apoptotic cells or debris, release of cytokines/chemokines and changes in the surface antigen profile. Furthermore, pro-inflammatory microglia release a wide range of soluble factors, dependent on the kind of stimulation, such as superoxide, nitric oxide (NO) and tumor necrosis factor α (TNFα) acting toxic against pathogens. Signals leading to activation include products of microorganisms, environmental toxins and protein aggregates (Hanisch, 2002; Zhou *et al.*, 2005). In their activated state microglia upregulate several surface molecules such as CD14, major histocompatibility complex (MHC) molecules, complement receptors and chemokine receptors (Rock *et al.*, 2004). Microglia express nine different toll like receptors (TLR 1-9) which are for example involved in detecting microbial infections like lipopolysaccharide (LPS), a component of gram-negative bacteria, lipoproteins, peptidoglycans and double-stranded RNA (Tsan and Gao, 2004; Garden and Möller, 2006). Furthermore, microglia upregulate metabotrophic P2 receptors to recognize signals from damaged cells like the nucleotides adenosintriphosphate (ATP) and uridintriphosphate (UTP; Napoli and Neumann, 2009). Upon immunological stimuli or in response to brain injuries microglia migrate along a chemokine gradient towards the stimuli (Cartier *et al.*, 2005) and phagocytose dead cells and debris. The best studied “eat-me” signal coming from apoptotic cells is the phospholipid phosphatidylserine (PtdSer) which is normally located within the inner cell membrane. The location of PtdSer to the outer membrane as result of the apoptotic process serves as signal for recognition of these cells by phagocytes and their ingestion (Ravichandran, 2003).

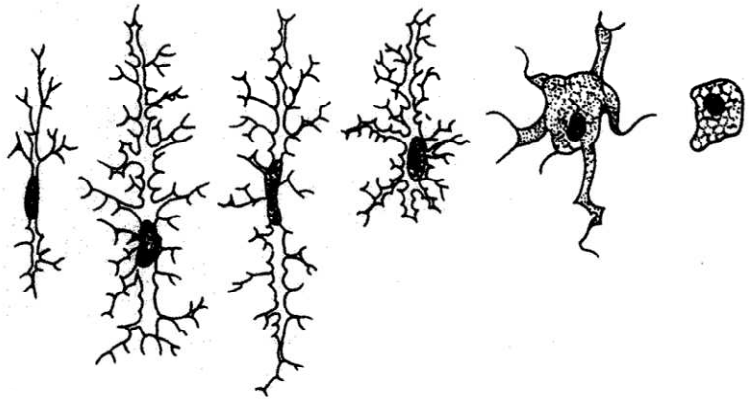

Fig.1.2: Morphology of microglia. Ramified microglia transform into an activated microglial cell (left to right). Modified from Kreutzberg, 1996.

1.1.4 Sources of microglia

Microglial function is often studied on primary microglia from rodents. These cells can be isolated and enriched from mixed glial cultures by a shaking procedure (Giulian and Baker, 1986). Optionally, a pure population of microglial cells can be obtained using a combination of density gradients and flow cytometric sorting (Ford *et al.*, 1995). This methodology was also applied to isolate human microglia post-mortem. Brain tissue from autopsy patients was used to isolate microglia by density gradient and magnetic-activated cell sorting (Olah *et al.*, 2012; Melief *et al.*, 2012). However, very limited numbers of primary microglia obtained from rodents and humans complicate classical biochemistry studies, systematic screening tests or cell therapy approaches. To circumvent these difficulties, mouse and human microglial lines were developed to substitute primary microglia. Murine cultured microglia were immortalized after infection with v-raf/v-myc recombinant retroviruses. The obtained BV2 cell line showed properties like macrophages in terms of antigen profile and phagocytic capacity (Blasi *et al.*, 1990, Bocchini *et al.*, 1992). Later on, immortalized human microglial lines were developed by transfection of embryonic brain-derived macrophages with the SV40 virus (Janabi *et al.*, 1995). Furthermore, the human microglial line HMO6 was generated through retroviral transformation of human embryonic telencephalon with v-myc (Nagai *et al.*, 2001; Nagai *et al.*, 2005). However, due to the transformation process these cells showed an altered cytokine profile and changes in their migratory capacity (Horvath *et al.*, 2008, Napoli *et al.*, 2009). Therefore, microglia derived from embryonic stem cells could provide a new tool to study microglial function *in vitro* and *in vivo*.

1.2 Induced pluripotent stem cells

Among stem cells, embryonic stem cells (ESC) have an enormous potential for biomedical approaches due to their capability of unlimited self-renewal and possibility to generate every cell type of an embryo. In 1998, the first human ESC line was generated by Thomson and colleagues (Thomson *et al.*, 1998). Human ESC were isolated from the inner cell mass of an embryo from *in vitro* fertilization. Since 2001, more than 70 human ESC lines were already generated.

Huge effort has gone into the development of functional equivalents of human ESC to overcome the ethical issue that a human embryo has to be destroyed. Takahashi and Yamanaka (2006) concentrated on the identification of pluripotency inducing factors. In 2006, they identified 24 candidates that were thought to be involved in maintaining pluripotency (Takahashi and Yamanaka, 2006). Using viral co-transduction of these factors, they generated the first cell lines with an embryonic-like state called induced pluripotent stem (iPS) cells. Further experiments demonstrated that overexpression of the four factors octamer 4 (Oct4), SRY box-containing gene 2 (Sox2), Krüppel-like factor 4 (Klf4) and c-Myc is sufficient to reprogram murine fibroblasts. Using the same factors different groups succeeded in the generation of iPS cells from human adult fibroblasts (Takahashi *et al.*, 2007, Yu *et al.*, 2007). In general, iPS cells show similarities to ESC in terms of morphology, proliferation, teratoma formation and expression of pluripotency markers such as stage-specific embryonic antigen (SSEA)-3, SSEA-4, Tra1-60 and Tra1-81. Furthermore, iPS cells can be cultivated for extended periods and maintain a normal karyotype. In the absence of self-renewal factors, iPS cells differentiate spontaneously into embryoid bodies (EB) thus being able to build every somatic cell type of the organism. Teratoma formation is the gold standard test of pluripotency. IPS cells are injected into a tetraploid blastocyst and contribute to the generation of an entire living organism (Kang *et al.*, 2009; Zhao *et al.*, 2009). For human iPS cells, the system is conducted in mice showing a severe combined immunodeficiency (SCID) affecting both B- and T-lymphocytes. Human iPS cells form teratomas comprising cells of all three germ layers (Takahashi *et al.*, 2007, Yu *et al.*, 2007). Immunohistochemistry analysis of cardiomyocytes confirmed the generation of the mesoderm whereas ectodermal and endodermal formation can be demonstrated using markers for neurons and pancreatic cells, respectively.

Due to their potential to generate every somatic cell type, iPS cells could be a useful instrument in regenerative medicine especially when generated from patients. Recently, different groups succeeded in the generation of disease-specific iPS cell lines from patients suffering from amyotrophic lateral sclerosis (Dimos *et al.*,2008), Parkinson's disease (Soldner *et al.*, 2009) and a variety of genetic diseases including Huntington's disease (Park *et al.*, 2008). Human iPS cells derived from patients can be used not only for drug screening but also to

investigate the pathology of the disease. Furthermore, the differentiation of iPS cells into the disease-affected cell type could be an approach for regenerative medicine.

1.3 Amyotrophic lateral sclerosis

Amyotrophic lateral sclerosis (ALS) is a late onset neurodegenerative disease with an incidence in Europe and Northern America of 1.9 per 100 000 population per year (Worms, 2001). Clinical symptoms include progressive muscular paralysis due to the degeneration of upper and lower motor neurons in the primitive motor cortex, brainstem and spinal cord, increased spasticity and hyper-reflexia (Rowland and Schneider, 2001; Glass *et al.*, 2010). The median disease onset is with 55 years with a survival of 2-5 years after onset of symptoms. So far, ALS is fatal since no cure is available. Approximately 90 % of ALS cases are sporadic whereas 10 % are inherited (familial ALS). In sporadic and familial ALS the same neurons are affected thus they are indistinguishable by symptoms, but onset and duration of the disease vary (Boillee *et al.*, 2006a).

1.3.1 Role of superoxide dismutase 1 in ALS

Dominant mutations in the gene encoding for superoxide dismutase 1 (SOD1) are the most common cause of familial ALS (Rosen *et al.*, 1993). So far, more than 114 mutations of SOD1 leading to ALS are known. SOD1 is a ubiquitously expressed homodimeric enzyme consisting of 153 amino acids with a stabilizing zinc ion and a catalytic copper ion in each subunit (Andersen, 2006). SOD1 catalyzes the reduction of superoxide to hydrogen peroxide which is further reduced to water by glutathione peroxidase. Transgenic mice overexpressing mutated SOD1 (mSOD1) develop progressive motor neuron disease similar to symptoms observed in humans (Gurney *et al.*, 1994; Wong *et al.*, 1995; Bruijn *et al.*, 1997). Thus, they can serve as animal models to study SOD1-mediated ALS. Toxicity of mSOD1 is non-cell autonomous. Mice expressing mSOD1 only in neurons (Pramatarova *et al.*, 2001; Lino *et al.*, 2002) or glial cells (Gong *et al.*, 2000) do not develop ALS.

Experiments with mice clearly demonstrated that toxicity of mSOD1 is not due to a loss of enzyme activity as mice lacking SOD1 do not develop motor neuron

degeneration (Reaume *et al.*, 1996). Furthermore, SOD1 toxicity is neither affected by reduced nor increased SOD1 wildtype activity (Bruijn *et al.*, 1998; Jaarsma *et al.*, 2001). Thus, mSOD1 has to cause disease through toxic properties. Different mechanisms involved in the toxicity of mSOD1 have been suggested. Catalytic copper is essential for SOD1 activity. It is loaded onto SOD1 by a copper chaperone for SOD1 (CCS) since free copper is toxic (Furukawa *et al.*, 2004). Inefficient incorporation onto SOD1 or impaired shielding of the ion due to abnormal SOD1 structure could lead to cellular damage and motor neuron degeneration. Mice deficient for CCS showed reduced amount of copper-loaded SOD1, but onset and progression of ALS in mSOD1 mice was not modified (Subramaniam *et al.*, 2002).

Cytoplasmic protein accumulations of insoluble proteins were detected in sporadic and familial ALS patients as well as mSOD1 mouse models in the affected tissue (Watanabe *et al.*, 2001; Furukawa *et al.*, 2006). Those aggregates contain ubiquitin (Watanabe *et al.*, 2001), a protein which labels proteins for degradation via the proteasome complex. Thus, protein accumulation could impair normal protein degradation and affect proteasome machinery.

Another feature found in ALS are morphological alterations of mitochondria such as vacuolated degeneration (Liu *et al.*, 2004) and changes in enzyme activities (Jung *et al.*, 2002; Li *et al.*, 2010). It was shown that mSOD1 is recruited to mitochondria only in the affected tissue and that this is independent of CCS and dismutase activity (Liu *et al.*, 2004). Furthermore, accumulation of mSOD1 with mitochondria is accompanied by a damage of mitochondrial bound proteins. The mitochondrial genome encodes only for 13 of the 1500 proteins required for mitochondrial function. Most of the proteins are nucleus encoded and have to be transported from the cytoplasma into the mitochondria (Boillee *et al.*, 2006a). Thus, association of mSOD1 with mitochondria could interfere with protein import and influence mitochondrial enzyme activity (Liu *et al.*, 2004).

Another mechanism involved in mSOD1-mediated toxicity might be alterations in reactive oxygen (ROS) production. Increased ROS levels were found in the brain and spinal cord of mSOD1 mice (Harraz *et al.*, 2008). The enzyme complex nicotinamide adenine dinucleotide phosphate (NADPH) oxidase is a source of ROS production. Experiments with mice expressing mSOD1 demonstrated that SOD1 regulates NADPH oxidase-dependent superoxide production. SOD1 can

regulate the activity of one subunit of the NADPH oxidase. However, this regulation is defective in mSOD1 leading to increased superoxide levels (Harraz *et al.*, 2008).

1.3.2 Role of microglia in ALS

Microglial activation was detected in the brain and spinal cord of ALS patients (Engelhardt and Appel, 1990; Henkel *et al.*, 2004) and mSOD1 mouse models (Hall *et al.*, 1998; Henkel *et al.*, 2006). An inflammatory response including microglial activation is initiated before the onset of the disease (Hall *et al.*, 1998). A pathological role of microglia in ALS was suggested based on data of animal models. Silencing of mSOD1 in neurons extended survival by slowing disease onset whereas inactivation of mSOD1 in microglia slowed disease progression (Boillee *et al.*, 2006b). Another study using PU.1-deficient mice which lack myeloid and lymphoid cells including microglia demonstrated also the involvement of microglia in ALS (Beers *et al.*, 2008). On the one hand, PU.1-deficient mice received bone marrow transplants from mSOD1 mice resulting in donor-derived microglia. No induction of motor neuron injury was induced in these mice. On the other hand, PU.1-deficient mice crossed with mSOD1 mice received bone marrow transplants from wildtype animals. A slowed motor neuron loss and prolonged disease duration and survival were observed in these mice. Both studies indicate that neurons are involved in the onset of the disease whereas microglia accelerate disease progression.

Wildtype microglia act less neurotoxic on motor neurons than mSOD1 microglia (Beers *et al.*, 2008). Microglia expressing mSOD1 were shown to produce more ROS and induce neuronal death. Coculture experiments of rat motor neurons with microglia activated with LPS or immunoglobulin G complexes from ALS patients demonstrated induced motor neuron injury. Furthermore, this effect could be prevented by an iNOS inhibitor demonstrating the involvement of NO in this process (Zhao *et al.*, 2004). In addition, mSOD1 affects microglial release of pro-inflammatory cytokines. Adult microglia expressing mSOD1 were shown to produce higher TNFα levels after stimulation with LPS in comparison to wildtype cells. However, neonatal microglia showed no difference in TNFα production after LPS stimulation (Weydt *et al.*, 2004). A recent publication further demonstrated a transformation of mSOD1 microglia from a neuroprotective to a neurotoxic

phenotype (Liao *et al.*, 2012). While microglia isolated from ALS mice at disease onset were neuroprotective and enhanced motor neuron survival, microglia from end-stage of the disease were neurotoxic leading to motor neuron death. These findings suggest an increased cytotoxic potential of adult microglia expressing mSOD1.

1.4 Aim of the study

Microglia are the first line of the innate immunity in the CNS involved in tissue homeostasis and host defence. However, there are some evidences that microglia are involved in neurodegenerative diseases like Alzheimer's disease, Huntington's disease and amyotrophic lateral sclerosis. Therefore, detailed studies about microglial function are crucial. Primary microglia or microglial lines obtained by viral transformation are often used for investigation of microglial function. However, primary microglia are only available in limited numbers complicating most studies while microglial lines might not reflect microglial behavior due to the transformation process.

The first aim of this study was to generate human microglial cell lines (iPSdM) derived from induced pluripotent stem cells. Microglial functionality was investigated regarding phagocytosis capacity, induction of pro-inflammatory cytokines and migratory potential towards chemokines.

Next, microglial role in SOD1-mediated ALS was investigated. IPSdM were transduced with wildtype and three different mutant SOD1 (G37R, G85R and G93A). Wildtype and mSOD1 expressing cells were compared regarding upregulation of pro-inflammatory cytokines, mitochondrial enzyme activities and ROS production.

2 Materials and Methods

2.1 Materials

2.1.1 Animals and cells

mouse strains

Rag2/IL-2R KO mice (C57BL/10SgSnAi[KO]γc-[KO]Rag2)	NIAID, USA (Cao *et al.*, 1995)

cell lines

HEK293FT	Invitrogen GmbH, Germany
Murine embryonic fibroblasts (MEF)	isolated from CD1 mice (E14.5); kindly donated by Anke Leinhaas, University of Bonn, Germany
iLB-C-35m-r1	generated and kindly provided by AG Brüstle, University of Bonn, Germany
iPS(foreskin)-1	WiCell Research Institute, USA

2.1.2 Plasmids

PLP1	Invitrogen GmbH, Germany
PLP2	Invitrogen GmbH, Germany
PLP3	Invitrogen GmbH, Germany
Pll3.7 PGK-eGFP	designed and modified by Isabella Napoli, AG Neumann
Pll3.7 PGK-hSOD1 wt-eGFP Pll3.7 PGK-hSOD1 G37R-eGFP Pll3.7 PGK-hSOD1 G85R-eGFP Pll3.7 PGK-hSOD1 G93A-eGFP	Plamids donated by AG Clement (University of Mainz) and modified by Johannes Friese (AG Neumann)

2.1.3 Primer

GAPDH_for	5’- CTG CAC CAC CAA CTG CTT AG -3’
GAPDH_rev	5’- TTC AGC TCA GGG ATG ACC TT -3’
TNFα_for	5’- GAC AAG CCT GTA GCC CAT GT -3’
TNFα_rev	5’- AGG ACC TGG GAG TAG ATG AGG -3’

iNOS_for	5’- CAG CTG GGC CGT GCA AAC CT -3’
iNOS_rev	5’- TGG CAC GGC TGG ATG TCG GA -3’

2.1.4 Chemicals and Reagents

1,4-Diazobicyclo-(2.2.2)octan	Sigma Aldrich Chemie GmbH, Germany
Alfazyme	PAA Laboratories GmbH, Austria
Amyloid-β	Bachem, Germany
β-Mercaptoethanol	Chemicon Europe, Germany
B27 supplement (50x)	Gibco, Invitrogen GmbH, Germany
Bovine serum albumin	Sigma Aldrich Chemie GmbH, Germany
Collagenase Type IV	Gibco, Invitrogen GmbH, Germany
ddH_2O	autoclaved and filtered in the Institute
D-(+)-Glucose solution (45 %)	Sigma Aldrich Chemie GmbH, Germany
Dimethyl sulfoxide	Sigma Aldrich Chemie GmbH, Germany
DMEM/F12 (1:1) with L-glutamine and 15 mM HEPES	Gibco, Invitrogen GmbH, Germany
DMEM with L-glutamine, w/o sodium pyruvate, with 4.5 g/l D-glucose	Gibco, Invitrogen GmbH, Germany
EDTA	Carl Roth GmbH & Co KG, Germany
Ethanol	Carl Roth GmbH & Co KG, Germany
Fluoresbrite Polychromatic Red microspheres 1.0 µm	Polyscience, Inc., Germany
Fibronectin from bovine plasma	Sigma Aldrich Chemie GmbH, Germany
Fibronectin 0.1 % solution	Sigma Aldrich Chemie GmbH, Germany
Fetal calf serum (FCS)	Gibco, Invitrogen GmbH, Germany
Gelatine from porcine skin	Fluka, Sigma Aldrich Chemie GmbH, Switzerland
Glutardaldehyd	Sigma Aldrich Chemie GmbH, Germany
Glycerol	Sigma Aldrich Chemie GmbH, Germany
Knockout serum replacement (KO/SR)	Gibco, Invitrogen GmbH, Germany
Laminin	Sigma Aldrich Chemie GmbH, Germany
L-Glutamine (200 mM)	Gibco, Invitrogen GmbH, Germany
LPS	Sigma Aldrich Chemie GmbH, Germany
LPS	Enzo Life Sciences GmbH, Germany

Mowiol 4-88	Kremer Pigmente, Germany
Non-essential amino acids (10 mM)	Gibco, Invitrogen GmbH, Germany
N2 supplement (100x)	Gibco, Invitrogen GmbH, Germany
Normal goat serum	Sigma Aldrich Chemie GmbH, Germany
Paraformaldehyde	Merck KgaA, Germany
PBS	Gibco, Invitrogen GmbH, Germany
Penicillin/Streptomycin	Gibco, Invitrogen GmbH, Germany
Poly-L-Lysine	Sigma Aldrich Chemie GmbH, Germany
Poly-L-Ornithin	Sigma Aldrich Chemie GmbH, Germany
ROCK Inhibitor Y-27632	Calbiochem, UK
Saccharose	Carl Roth GmbH & Co KG, Germany
Sialidase (1 U)	Roche, Germany
Sodium pyruvate (100 mM)	Gibco, Invitrogen GmbH, Germany
Tissue Tek, O.C.T.TM compound	Sciences Service GmbH, Germany
Tris	Carl Roth GmbH & Co KG, Germany
TritonX	Sigma Aldrich Chemie GmbH, Germany
Trypsin (0.25 %)	Gibco, Invitrogen GmbH, Germany

2.1.5 Growth Factors and Cytokines

Recombinant human fibroblast growth factor 2 (rhFGF2)	R&D Systems GmbH, Germany
Recombinant human granulocyte-macrophage colony stimulating factor (rhGM-CSF)	Gibco, Invitrogen GmbH, Germany
Recombinant human interferon γ (rhIFNγ)	R&D Systems GmbH, Germany
Recombinant human tumor necrosis factor α (rhTNFα)	R&D Systems GmbH, Germany
Recombinant human CX3CL1/Fractalkine full length	R&D Systems GmbH, Germany

2.1.6 Buffers and Solutions

0.01 M sodium citrate buffer, pH 6	5.88 g Tri-sodium citrate (dihydrate) ad 2 l aqua bidest. adjust pH with 1 M HCl 1 ml Tween 20
Krebs-Hepes-buffer pH=7.4	1.98 g Hepes 7.60 g NaCl 0.42 g KCl 0.29 g $CaCl_2$ 0.049 g $MgCl_2$ 1.98 g glucose ad 1 l aqua bidest.
Mowiol	4.8 g Mowiol 4-88 12 g Glycerol 24 ml 0.2 mM Tris buffer, pH 8.5 1.32 g 1,4-Diazobicyclo-(2.2.2)octan 12 ml aqua bidest.
Gelatine	0.5 g in 500 ml aqua dest.
Poly-L-Ornithin (0.01 mg/ml)	9.2745 g boric acid ad 1 l aqua dest. 100 mg Poly-L-Ornithin
Saccharose, 30 %	30 % saccharose 0.1 % sodium azide ad 500 ml PBS

2.1.7 Kits

Lipofectamin 2000	Invitrogen GmbH, Germany
RNeasy Mini Kit	Quiagen, Germany
SuperScript First-Strand Synthesis System	Invitrogen GmbH, Germany
SYBR green	Invitrogen GmbH, Germany
Colorimetric MTT Kit	Millipore Corporation, USA

2.1.8 Media

MEF-medium	DMEM with L-glutamine, without Na-pyruvat, 4.5 g/l D-glucose 0.1 mM NEAA 1 mM sodium pyruvate 2 mM L-glutamine 10 % FCS
iPS-medium	DMEM/F12 (1:1) with L-glutamine with HEPES (15 mM) 20 % knockout serum replacement 0.1 mM NEAA 0.1 mM L-glutamine 0.1 mM β-mercaptoethanol 25 ng/ml rhFGF2
differentiation medium	DMEM/F12 (1:1) with L-glutamine with HEPES (15 mM) 20 % knockout serum replacement 0.1 mM NEAA 0.1 mM L-glutamine
B27-medium	DMEM/F12 (1:1) with L-glutamine with HEPES (15 mM) 2 % B27 0.2 mM L-glutamine 15.6 µg/ml D-glucose 20 ng/ml rhFGF2 5 µg/ml fibronectin
N2-medium	DMEM/F12 (1:1) with L-glutamine with HEPES (15 mM) 1 % N2 supplement 0.5 mM L-glutamine 15.3 µg/ml D-glucose 100 µg/ml penicillin/streptomycin
freezing medium	50 % FBS 40 % medium 10 % DMSO

2.1.9 Antibodies

Primary antibodies

Antigen	Reactivity	Host	Company
CD11b	mouse, human	rat	BD Pharmingen, Germany
CD11c-Bio	mouse, human	hamster	BD Pharmingen, Germany
CD14	human	mouse	Exbio, Czech Republic
CD16/32 (Fc block)	mouse, human	rat	BD Pharmingen, Germany
CD16/32-Bio	mouse, human	rat	BD Pharmingen, Germany
CD29	mouse, human	rat	BD Pharmingen, Germany
CD34	human	mouse	Exbio, Czech Republic
CD36	mouse, human	mouse	BD Pharmingen, Germany
CD40	human	mouse	Exbio, Czech Republic
CD45	mouse, human	rat	BD Pharmingen, Germany
CD49d	mouse, human	rat	BD Pharmingen, Germany
CD68	mouse, human	rat	Serotec, USA
CD86	mouse, human	rat	BD Pharmingen, Germany
CD206	human	mouse	Acris, Germany
CX3CR1	mouse, human	rabbit	ProSci Incorporated
I-A/I-E-Bio (MHC class II)	mouse, human	rat	BD Pharmingen, Germany
GFAP	mouse	rabbit	Dako, Germany
GFP		mouse	Chemicon, Germany
Iba1	mouse, human	rabbit	Wako, Germany
Nestin	human	mouse	Millipore, USA
Siglec-11-Bio	human	goat	R&D Systems GmbH, Germany
SOD1	human, rat	rabbit	Wako, Germany
TUJ1	human	rabbit	Covance, USA
isotype IgG1 κ		mouse	BD Pharmingen, Germany
isotype IgA		mouse	BD Pharmingen, Germany
isotype IgG2aκ		rat	BD Pharmingen, Germany
isotype IgG2bκ		rat	BD Pharmingen, Germany

isotype IgG1-Bio	armenian hamster	eBioscience, USA
isotype IgG2aκ-Bio	rat	BD Pharmingen, Germany
isotype IgG2bκ-Bio	rat	BD Pharmingen, Germany

Additional staining reagents

4',6-diamidino-2-phenylindole (DAPI)	Sigma Aldrich Chemie GmbH, Germany
dihydroethidium (DHE)	Invitrogen GmbH, Germany

Secondary antibodies

Fluorophore	Reactivity	Host	Company
Phycoerythrin	mouse	goat	Jackson Immunoresearch, UK
Phycoerythrin	rat	goat	Jackson Immunoresearch, UK
Phycoerythrin	rabbit	goat	Jackson Immunoresearch, UK
Phycoerythrin-Streptavidin	Biotin	goat	Jackson Immunoresearch, UK
Alexa488	mouse	goat	Invitrogen GmbH, Germany
Alexa488	rabbit	goat	Invitrogen GmbH, Germany
Cy3	rabbit	goat	Dianova, Germany
Cy3	rat	goat	Dianova, Germany
Cy3-Streptavidin	Biotin	goat	Dianova, Germany

2.1.10 Consumable supplies

6-well Tissue Culture Plate	Cellstar, Greiner Bio One, Germany
8.0 µm Culture Plate Inserts 12 mm Diameter	Millipore, Germany
Bacterial dishes (100 mm)	Becton Dickinson GmbH, Germany
Corning Cell Scraper	Sigma Aldrich Chemie GmbH, Germany
Cell strainer	Becton Dickinson GmbH, Germany
Cryovials (2 ml)	Nunc GmbH & Co KG, Germany
Tissue Tek, Disposable Vinyl Specimen Molds	Sciences Services GmbH, Germany

Falcon tubes (15 ml)	Cellstar, Greiner Bio One, Germany
Falcon tubes (50 ml)	Sarstedt Ag & CoKG, Germany
Filtropur (0.25 µm, 0.4 µm)	Sarstedt Ag & CoKG, Germany
Graduate pipette Tipps (10 µl, 100 µl, 1000 µl)	Starlab GmbH, Germany
Lab-Tek Chamber Slide w/ Cover Permanox Slide Sterile 4 Well	Labomedic, Germany
Latex gloves	Ansell Healthcare Europe NV, Belgium
Microscope cover glasses	P. Marienfeld GmbH, Germany
Needles	Sterican, Braun Meisungen AG, Germany
Nitrile gloves	Ansell Healthcare Europe NV, Belgium
Pasteur pipettes	Brand GmbH & Co KG, Germany
Pipettes (5 ml, 10 ml, 25 ml)	Sarstedt AG & Co KG, Germany
Safe-seal micro tubes (0.5 ml, 1.5 ml, 2 ml)	Sarstedt Ag & Co KG, Germany
Syringes (5 ml, 10 ml)	Omnifix, Braun Meisungen AG, Germany
Tissue Culture Dishes (35 mm, 60 mm, 100 mm)	Sarstedt Inc., USA
Vacuum driven disposable bottle top filter	Millipore Corporation, USA

2.1.11 Technical equipment

- 20℃ freezer	Liebherr, Bulle, Switzerland
+ 4℃ fridge	Liebherr, Bulle, Switzerland
BD FacsCalibur	BD Bioscience, Germany
Cell MateII (pipette boy)	Thermo Fisher Scientific Inc., USA
Confocal Microscope	Olympus, Germany
Envision 2104 Multilabel Reader	Perkin Elmer, USA
Eppendorf Mastercycler epgradient S	Eppendorf, Germany
Hera cell 150 (incubator)	Heraeus Holding GmbH, Germany
Hera freeze (-80℃ freezer)	Heraeus Holding GmbH, G ermany
Hera safe (laminar-air flow workbench)	Kendro Laboratory Products GmbH, Germany
Mefaguge1.0R (centrifuge)	Heraeus Holding GmbH, Germany

Microscopes	Carl Zeiss AG, Germany
HBO 50/AC	
Axiovert200M	
ImagerZ1	
Fluoview FV1000	Olympus
Microtom HM 560 M	Microm International, Germany
Pipettes (10 µl, 100 µl, 1000 µl)	Eppendorf AG, Germany
Systec D-150 (autoclave)	Systec GmbH, Germany
Thermomixer compact	Eppendorf AG, Germany
Water bath WB/OB7-45	Memmert GmbH & CoKG, Germany

2.1.12 Software

Cell Quest Pro	BD Bioscience, USA
FlowJo	TreeStar, USA
ImageJ 1.43m	National Institute of Health, USA
Olympus Fluoview FV1000	Olympus, Germany
SPSS	IBM, Germany
Wallac Envision Manager 1.12	Dazdaq, UK

2.2 Methods

2.2.1 Generation of induced pluripotent stem cell derived microglial precursors (iPSdM)

For maintenance and expansion of human induced pluripotent stem (iPS) cells, cells were cultured in chemically defined medium in the presence of 10 ng/ml rhFGF2 on a mouse embryonic fibroblast layer. Cells were detached using collagenase IV, collected in a tube and centrifuged at 800 rpm for 3 min. Cell pellet was resuspended in differentiation medium and cultivated on non-adherent bacterial dishes to induce embryoid body (EB) formation. EBs were kept in suspension for 8 days for spontaneous differentiation. EBs were plated on poly-L-ornithin / fibronectin - coated dishes and allowed to attach for 2 days. Neural precursors were selected for 14 days in B27-medium supplemented with 20 ng/ml rhFGF2 and 5 µg/ml fibronectin. Medium was changed to N2-medium supplemented with 20 ng/ml rhFGF2 and 10 ng/ml laminin. Differentiation of microglial precursors was initiated by withdrawal of the growth factors after 10 days of expansion. After 160 days of differentiation, first microglial precursors appeared in the culture identified by morphology. To enhance cell proliferation 100 ng/ml rhGM-CSF were added to the media after the development of the first microglial precursors. Microglial precursors were mechanically isolated with a micropipette under microscope and cultivated at high density on poly-L-lysin - coated dishes in N2-medium supplemented with 100 ng/ml rhGM-CSF. After several days in culture, microglial precursor cells started to proliferate. Microglial precursors proliferated without the addition of growth factors after some passages and could be cultivated in N2-medium on non-coated cell culture dishes. Cells could be passaged 1:3 till 1:5 twice a week. In total, 4 iPS-derived microglial precursor (iPSdM) lines out of two different iPS cell lines were generated. IPSdM line 1 and 4 are derived from iLB-C-35m-r1 and line 2 and 3 from iPS(foreskin)-1.

2.2.2 Maintenance of iPSdM

IPSdM were cultivated in N2-medium at 5 % CO_2 at 37°C. Upon 80-90 % confluency, cells were split 1:3 till 1:5 twice a week using 0.25 % trypsin. IPSdM could be frozen slowly in N2-medium supplemented with 10 % DMSO and 50 % FCS.

2.2.3 Proliferation assay

For proliferation assay, 200 000 cells were seeded in 6 cm dishes in N2-medium. Total cell number was counted after 24 h, 48 h, 72 h and 96 h using a Neubauer chamber.

2.2.4 Analysis of cell viability

MTT (3-(4,5-dimethylthiazol-2-yl)-2,5-dipenyl tetrasodium bromide) assay was used to check for cell viability. 50 mg of the MTT reagent were diluted in 10 ml PBS, pH 7.4. For detection 15 000 cells were seeded in a 96-well flat bottomed tissue culture plate in N2-medium with a final volume of 100 µl. Cells were incubated at 37℃, 5 % CO_2. On the next day, 10 µl MTT dilution were added into each well and mixed by tipping to the plate. After 4 h incubation at 37℃, 5 % CO_2, 100 µl of 0.04 M HCl in isopropanol were added into each well and mixed thoroughly. The absorbance at 570 nm and 630 nm (as reference) was measured using an ELISA reader.

2.2.5 Immunocytochemistry of cultured cells

For immunocytochemistry, human cultures and iPSdM were washed 3 x with PBS and then fixed with 4 % paraformaldehyde (PFA) for 10 min. Cultures were blocked with 10 % BSA, 5 % normal goat serum and for intracellular markers additionally with 0.1 % Triton X for 30 min at room temperature (RT). Human cells were stained with antibodies directed against Iba1 (1 µg/ml), CD45 (1 µg/ml), CD68 (2 µg/ml), SOD1 (1:250), nestin (2 µg/ml) and βIII-tubulin (clone TUJ1, 1 µg/ml). All primary antibodies were incubated over night at 4℃. Afterwards, cultures were washed 3 x for 5 min with PBS. Primary antibodies were detected with Cy3-conjugated goat-anti-rat (2.5 µg/ml), goat-anti-rabbit (2.5 µg/ml), Alexa488-conjugated goat-anti-rabbit (4 µg/ml) and goat-anti mouse (4 µg/ml). Secondary antibodies were incubated for 90 min at RT in the dark. Cultures were again washed 3 x for 5 min with PBS and counterstained with DAPI (0.1 µg/ml) for 30 s. After 3 x washing with PBS, cells were covered with Mowiol and cover slides. Stained cultures were stored at 4℃.

2.2.6 Flow cytometry

Cells were unstimulated or stimulated for 4 days with 1 µg/ml LPS or 1000 U/m IFNγ. After a 3 x washing period with PBS, cells were collected from the cell culture dish using a cell scraper. For Siglec-11 detection, cells were pre-incubated with sialidase (1:400) for 2.5 h in medium at 37℃ and 5 % CO_2. CD16/32 was used as Fc block (4 µg/ml) for cells stained with biotinylated antibodies adding 5 min before the first antibody. Cells were stained for 1 h at 4℃ using the following primary antibodies: CD11b (2.5 µg/ml), CD11c-Bio (2.5 µg/ml), CD14 (5 µg/ml), CD16/32-Bio (2.5 µg/ml), CD29 (2.5 µg/ml), CD34 (5 µg/ml), CD36 (2.5 µg/ml), CD40 (5 µg/ml), CD45 (2.5 µg/ml), CD49d (2.5 µg/ml), CD86 (2.5 µg/ml), CD206 (5 µg/ml), I-A/I-E-Bio (2.5 µg/ml) and CX3CR1 (2.5 µg/ml). The corresponding isotype control was used as control. After 3 x washing, cells were incubated with the secondary antibody for 30 min at 4℃ in the dark. Primary antibodies were detected with PE-conjugated goat-anti-mouse, goat-anti-rat, goat-anti-rabbit or PE-Streptavidin (2.5 µg/ml). Cells were washed again with PBS, diluted in 500 µl PBS and marker expression was analyzed using flow cytometry.

2.2.7 Western Blot Analysis

Western Blot analysis was done by AG Clement, University of Mainz. Cells were harvested in TBS extraction buffer containing 2 % SDS and 10 % sucrose and 4 x sonificated. BCA-based protein determination was performed according to manufacturer's protocol (Thermo Fisher). 12 µg of protein were separated on 12 % SDS-PAGE gels and transferred on nitrocellulose. Endogenous SOD1 and SOD1-GFP fusion proteins were detected by a rabbit monoclonal antibody from Epitomics and a corresponding HRP-coupled secondary antibody (Dianova). Enhanced luminescent signals were detected with the LAS3000 system (Fuji) and quantified by the ImageJ software.

2.2.8 Gene transcript analysis

For gene transcript analysis, 200 000 cells of iPSdM were seeded in 6 cm dishes and stimulated with either 1000 ng/ml LPS, 1000 U/ml rhIFNγ or 100 ng/ml rhTNFα. Unstimulated cells served as control. After 6 h of stimulation RNA was extracted using RNeasy Mini Kit. Right after the isolation reverse transcription was performed following the Invitrogen protocol for SuperScript First-Strand Synthesis

System. Transcribed cDNA was dilutet to 250 ng/µl. For real-time RT-PCR following mix was prepared in 96-well-plate: 12.5 µl SYBR Green Mix, 4 µl cDNA, 1 µl of each primer (10 pmol/µl) and 6.5 µl aqua dest. The same mix with aqua dest. instead of cDNA was used as non-template-control. Then, the plate was covered with a plastic lid and the following program was run:

Cover T° = 105°C

Initial denature:	95°C	10 min
Denature:	95°C	15 s
Annealing:	60°C	20 s
Elongation:	72°C	30 s
Amplification:	for 40 cycles	

To asses if a specific product was obtained a dissociation curve analysis was performed using the following program:

95°C	15 s
60°C	15 s
95°C	15 s
ramp rate 20 min	

2.2.9 Microsphere beads phagocytosis assay

To analyze microglial cells for phagocytosis capacity of beads, 100 000 cells per condition were seeded per well in 6-well-plates in 2 ml N2-medium and cultured at 37°C, 5 % CO_2. The next day, cells were stimulated with 500 ng/ml LPS or 1000 U/ml rhIFNγ for 24 h. Unstimulated cells were used as control. Cells were incubated with 5 µl microspheres beads for 30 min at 37°C, 5 % CO_2 and then detached using trypsin. After centrifugation at 1200 rpm for 3 min cells were resuspended in 500 µl PBS and analyzed using flow cytometry. Cells that had phagocytose more than 1 bead were taken into account.

2.2.10 Aβ phagocytosis assay

To analyze microglial cells for phagocytosis capacity of amyloid β, 40 000 cells per condition were seeded per well in chamber slides. Cells were kept unstimulated or stimulated with 500 ng/ml LPS or 1000 U/ml rhIFNγ for 24 h at 37°C, 5 % CO_2 and then incubated with biotinylated amyloid β (10 µg/ml) for 1.5 h at 37°C, 5 % CO_2.

Cells were stained for Iba1 and amyloid β as described above and percentage of phagocytosing cells was analyzed by fluorescence microscopy.

2.2.11 Migration assay

Cells were detached using trypsin and 100 000 cells per condition were seeded in the upper chamber of a transwell-system in medium to settle down. After 1 h cells were treated with different concentrations of rhCX3CL1 (0, 5, 10, 15 and 20 ng/ml) in the lower chamber for 4 h at 37℃, 5 % CO_2. As control for undirected migration 20 ng/ml rhCX3CL1 were added into both chambers. Using a cotton bud cells of the upper chamber were removed. Cells that had migrated to the lower chamber and to the backside of the membrane were counted. The count occurred under bright field and all 4 big squares of the Neubauer chamber were analyzed.

2.2.12 Detection of ROS by dihydroethidium

Cells were seeded with a density of 30 000 cells per well in chamber slides. Cells were stimulated for 24 h with 1000 ng/ml LPS, 1000 U/ml rhIFNγ or with 500 ng/ml rhTNFα for 20 min. To detect ROS production cells were washed 3 x with Krebs-HEPES-buffer and stained for 15 min at 37℃ with 30 µM dihydroehidium (DHE). Cells were washed again three times with Krebs-HEPES-buffer and fixated with 0.25 % glutaraldehyde in 4 % PFA. Cells were counterstained with DAPI (0.1 µg/ml) and mounted with Mowiol 4-88 and cover slides. Quantification was done using confocal microscopy and ImageJ. Per experiment and condition, 3 to 5 pictures were analyzed.

2.2.13 Mitochondrial analysis

Analysis was done by AG Kunz, University of Bonn. For analysis of complex I (NADH:CoQ 1 Oxidoreductase) the activity of rotenone-sensitive NADH:CoQ 1 oxidoreductase was measured at 30℃ using a dual-wavelength spectrophotometer (Aminco DW 2000, SLM Instruments, Rochester, NY) at 340-380 nm ($\varepsilon_{red\text{-}ox}$ = 5.5 mM^{-1} cm^{-1}) as described previously (Wiedemann *et al.*, 2000). The reaction medium contained of 50 mM KCl, 1 mM EDTA, 10 mM TRIS-HCl (pH 7.4), 1 mM KCN, 100 µM CoQ 1 and 150 µM NADH. The assay was initiated by addition of the sample and the velocity of NADH oxidation was

monitored. To determine the rotenone-insensitive NADH oxidation rate, 20 µM rotenone were added to the assay mixture after 2 min. Activities were determined as the differences between the total NADH oxidation rate and the rotenone-insensitive NADH oxidation rate. For analysis of complex IV (Cytochrome c Oxidase) the cytochrome c oxidase activities were measured at 30℃ in 0.1 M potassium phosphate buffer (pH 7.4) containing 0.02 % laurylmaltoside (Sigma, Deisenhofen, Germany) monitoring the oxidation of ferrocytochrome c in its band at the wavelength pair 510-535 nm using a dual wavelength spectrophotometer (Aminco DW 2000, SLM Instruments) as described previously (Wiedemann *et al.*, 2000). For citrate synthase analysis the activity of citrate synthase was determined at 30℃ by a standard method (Bergmeyer) . The protein content of the cell homogenates was determined using a protein assay kit based on Peterson's modification of the micro-Lowry method according to the instructions of the manufacturer (Sigma).

2.2.14 Virus production and transduction of iPSdM

For lentiviral production the plasmid with gene of interest was transfected together with three packaging plasmids (PLP1, PLP2, PLP3) into HEK293FT cells (done by Johannes Friese). For transfection, Lipofectamin 2000 was used following manual instructions. Medium was changed 16 h post-transfection. Supernatant was collected 48 h and 72 h after transfection. For transduction, iPSdM1 were seeded in 10 cm dishes in culture medium and viral particles were added to media for 3 days. In total, iPSdM1 were transduced 4 times with GFP, hSOD1 wt-GFP, hSOD1 G37R-GFP, hSOD1 G85R-GFP and hSOD1 G93A-GFP. Afterwards cells were sorted via FACS sorting using the GFP-tag.

2.2.15 Transplantation of GFP-iPSdM into immunodeficient mice

GFP expressing iPSdM were used for transplantation into 6 weeks old Rag2/IL-2R KO mice. Cells were detached using trypsin, centrifuged at 1200 rpm for 3 min and pellet was diluted in 1 % DNase containing cyto-buffer with a concentration of 150 000 cells/µl. Mice were anesthetized with Fentanyl, Midazolam and Medetomidin and Isofluran/O_2. Mice were fixed, sculls were shaved and 1 µl of the cell suspension was applied over 2 min in a 0.52 mm prepared borehole. Cells were transplanted into the left side of the hippocampus (coordinates referred to

Bregma: posterior 2.4/ lateral 1.5/ ventral 1.4-1.6). Afterwards, the borehole was fixed with bone wax, washed with antiseptic solution and the wound was closed with a stapler. To avoid inflammatory response mice received Carprofen (5 ng per g body weight). After 3 and 9 weeks mice were transcardially perfused with PBS following 4 % PFA. The brain was isolated and post fixated for 1 day in 4 % PFA and then cryoprotected in 30 % sucrose in PBS. Organs were embedded in TissueTek, stored at -80°C for 20 min and 20 µm cryosections were collected on glass slides. For detection, sections were stained as described above and analyzed using confocal microscopy.

2.2.16 Immunohistochemistry of brain slices

Brain slices were once washed with PBS for 5 min. Slices were blocked with 10 % BSA, 0.5 % normal goat serum and 0.1 % Triton X in PBS for 90 min at RT in a wet chamber. Cells were incubated with primary antibodies directed against CD68 (2 µg/ml), GFAP (1 µg/ml) and GFP (1:500) over night at RT. The next day, cells were washed 3 x with PBS for 5 min and incubated with the secondary antibodies Cy3-conjugated goat-anti-rabbit or goat-anti-rat (3 µg/ml) and Alexa488-conjugated goat-anti-mouse (2 µg/ml) for 2 h at RT in the dark. Slices were washed 3 x for 5 min with PBS and then counterstained with DAPI (0.5 g/l) for 10 min at RT. Slices were washed again with PBS and covered with Mowiol and cover slides and stored at 4°C.

2.2.17 Statistical analysis

Data are presented as mean ± SEM of at least 3 independent experiments. Data were analyzed by student t-test for two groups only or ANOVA for more than two groups using SPSS computer software.

3 Results

3.1 Generation and characterization of human microglial precursor lines

Microglia represent a crucial target for neuroimmunological research due to their manifold involvement in the pathology of neurodegenerative diseases. However, human primary microglia are only available in very limited numbers, thus classical studies are difficult to perform. Two human microglial cell lines were developed to overcome this problem (Janabi *et al.*, 1995; Nagai *et al.*, 2001; Nagai *et al.*, 2005). However, these cells might exhibit an altered cytokine profile and changes in their behavior due to the transformation process. Therefore, the aim of this work was to generate a protocol for the differentiation of human induced pluripotent stem (iPS) cells to microglial precursors.

3.1.1 Generation of microglial cells derived from human induced pluripotent stem cells (iPSdM)

Microglia develop during primitive haematopoiesis in the fetal yolk sac from immature macrophages (Ginhoux *et al.*, 2010; Prinz *et al.*, 2011; Saijo and Glass, 2011). A differentiation protocol allowing co-development of yolk sac-like macrophages and neural progenitors was developed to recapitulate this developmental program under culture conditions (Fig. 3.1).

Human iPS cells derived from adult skin or foreskin fibroblasts were used for the differentiation protocol. IPS cells were cultivated in a defined medium supplemented with FGF2 on an irradiated embryonic mouse fibroblast layer (Fig. 3.2 A). The morphology of iPS cells can differ depending on the species they are obtained from. Human iPS cells build circular, flat colonies with a well-defined shape. Losing their defined shape and building gaps in their colony structure is a sign for beginning of differentiation in these cells. To induce spontaneous differentiation, iPS cells were detached and cultivated on non-adherent dishes in the absence of a fibroblast layer and self-renewal factors. Embryoid bodies (EBs) differentiated spontaneously (Fig. 3.2 A), displaying a solid round structure. Seven days old EBs were stained positive for the neuronal precursor marker nestin and for the macrophage or microglial markers Iba1 and CD45, respectively (Fig. 3.1

and 3.2 B). Nestin positive cells were located next to CD45 and Iba1 positive cells indicating that at this stage neuronal cells as well as immature macrophages developed. EBs were plated on poly-L-ornithin and fibronectin-coated culture dishes in B27-medium supplemented with FGF2 and fibronectin to induce neural differentiation (Fig. 3.1 and 3.2 A). Cells started to grow out and were expanded in N2-medium supplemented with FGF2 and laminin. Differentiation of microglia was induced after withdrawal of FGF2. Microglial-like cells appeared as shiny round cells and developed within some weeks in a mixed culture of glial and neuronal cells (Fig. 3.1). CD45 positive microglial-like cells were found next to βIII-tubulin positive neuronal cells (Fig. 3.1 and 3.2 C). Microglial-like cells started to proliferate after some days. GM-CSF was added to the culture to enhance cell survival and proliferation (Fig. 3.1). Microglial-like cells could be isolated and expanded on cell culture dishes.

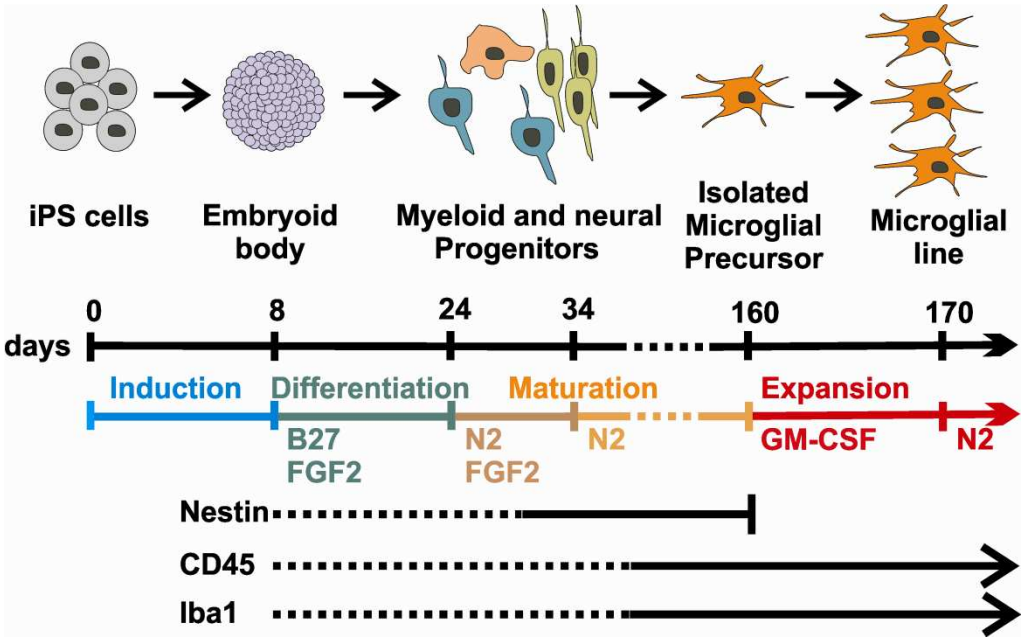

Fig. 3.1: Schematic drawing of the differentiation of human iPS cells to microglial precursors. Human iPS cells spontaneously differentiated within 8 days into embryoid bodies (EBs) on non-adherent dishes in the absence of FGF2. EBs were plated on extracellular matrix-coated dishes in B27-medium supplemented with FGF2 for 14 days. Neural and myeloid progenitors started to develop and were expanded for 10 days in N2-medium supplemented with FGF2. After withdrawal of FGF2, microglial precursors co-developed with neurons in N2-medium. Microglial precursors were mechanically isolated on day 160 and were expanded for 10 days in N2-medium supplemented with GM-CSF to obtain a microglial line on day 170 that stably proliferated in N2-medium without any growth factors.

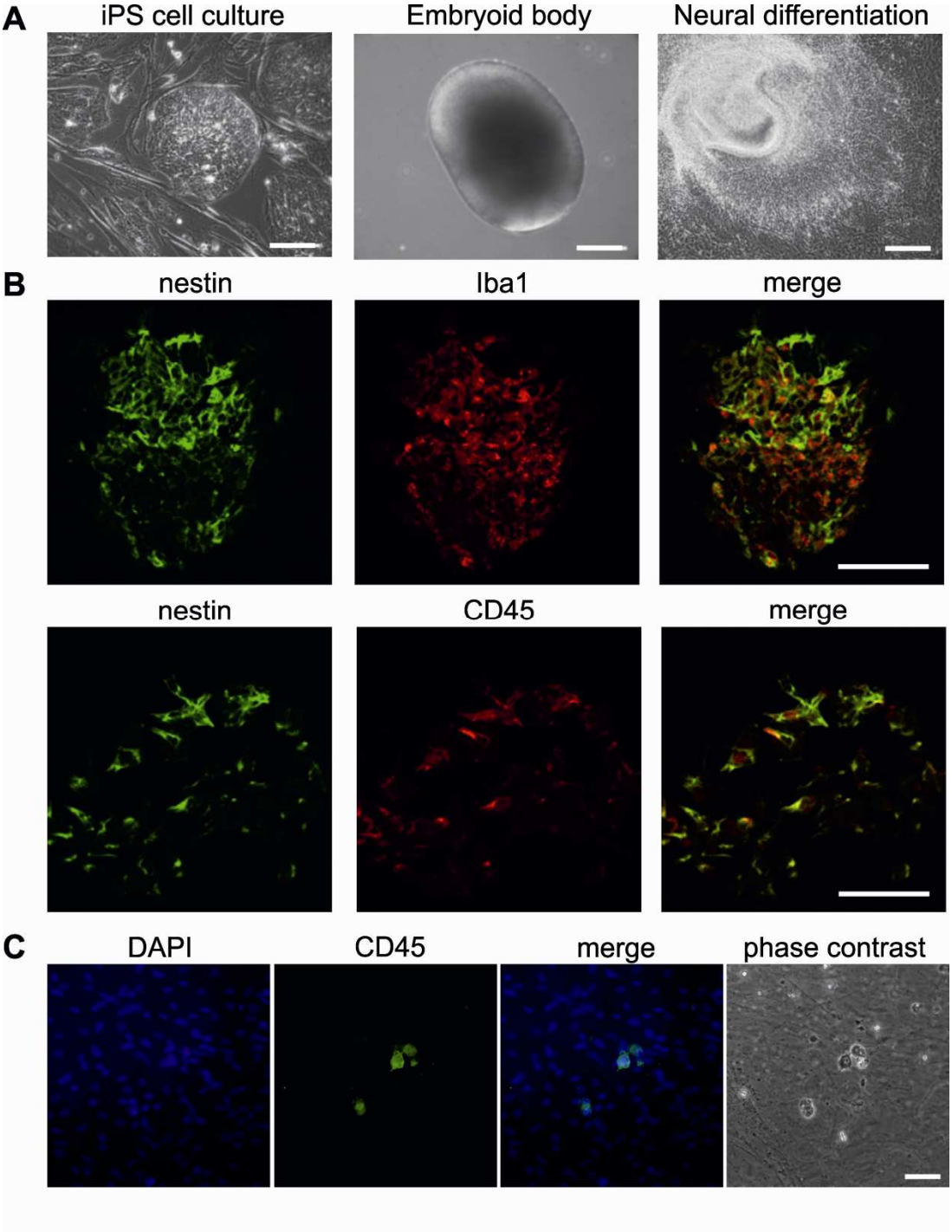

Fig. 3.2: Differentiation of iPS cells into microglial precursor. A. Phase contrast images from the differentiation procedure. Human iPS cells were cultured on an irradiated mouse embryonic fibroblast layer. IPS cells were detached and spontaneously differentiated into embryoid bodies (EBs). EBs were plated and differentiated into neural and myeloid progenitors. Scale bars: 100 µm. **B.** Immunofluorescence images of EBs. EBs were stained positive for nestin, Iba1 and CD45. Scale bars: 100 µm. **C.** Immunostaining of differentiation culture (maturation of myeloid cells) stained with an antibody directed against the myeloid marker CD45. CD45-positive cells were detected within DAPI stained cells. Phase contrast image shows these cells within a mixed culture. Scale bar: 50 µm.

3.1.2 Selection and generation of microglial lines

Cells with a microglial-like morphology developed about 4 month after withdrawal of FGF2 and started to proliferate after some days. These cells were round, with a bright shining cell body and could be distinguished from neurons by their comparatively bigger cell body and the absence of processes. Microglial-like cells were mechanically isolated and cultured at 80-90 % density in medium supplemented with GM-CSF to enhance cell survival. After some days cells started to proliferate and could be cultivated on cell culture dishes in N2-medium without additional growth factors. Twice a week iPS-derived microglial precursors (iPSdM) were passaged between 1:3 to 1:5. In total, four different microglial lines out of 2 different iPS cell lines could be generated. The iPS cell line iLB-C-35m-r1 was differentiated into iPSdM line 1 and 4 and the iPS(foreskin)-1 line was differentiated into iPSdM line 2 and 3.

Microglial identity could be confirmed via immunocytochemistry using antibodies directed against the microglial marker proteins Iba1 and CD68. A co-localized staining of Iba1 and CD68 could be detected throughout the cytoplasm (Fig. 3.3 A).

All four microglial lines showed a similar morphology. The phenotype of the microglial precursors varied from a ramified structure with several processes to a completely rounded cell morphology (Fig. 3.3 B). Microglial cells showed long-term proliferation and did not change their morphology until at least passage 25.

Proliferation assay was performed to characterize the growth rate of the iPSdM lines. A defined cell number of iPSdM was seeded and the cells were counted every 24 hours for a total of 4 days (Fig. 3.3 C). All four microglial lines showed similar growth behaviors with a mean doubling time of 24.6 ± 1.1 h (iPSdM1), 26.3 ± 2.0 h (iPSdM2), 27.1 ± 1.4 h (iPSdM3) and 25.4 ± 1.4 h (iPSdM4).

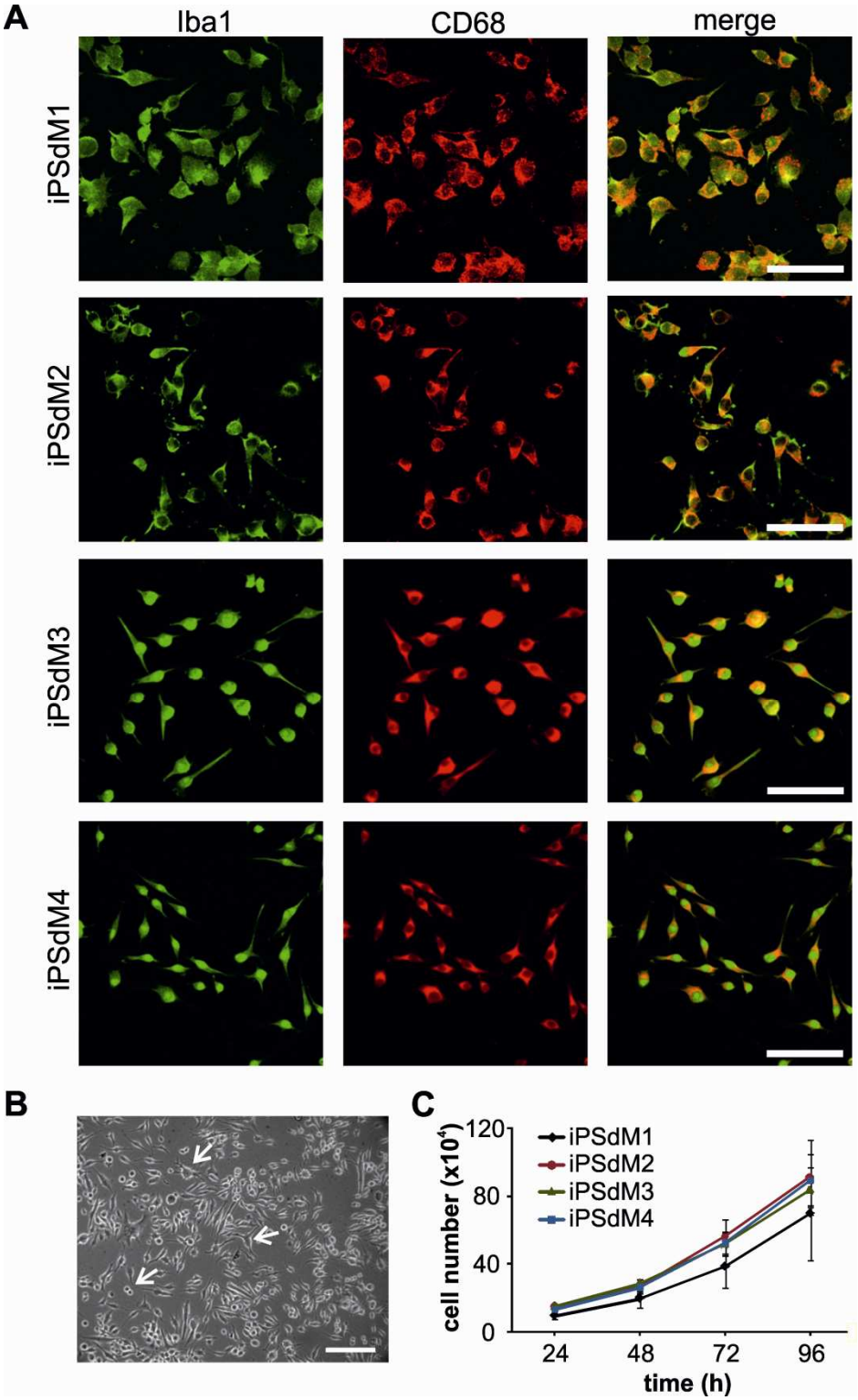

Fig. 3.3: Establishment of microglial precursor lines from iPS cells. A. Immunostaining of induced pluripotent stem cell derived microglial precursor (iPSdM) lines 1, 2, 3 and 4. Cells were stained positive for the microglial marker proteins Iba1 and CD68. Scale bars: 100 µm. **B.** Representative phase contrast image of iPSdM line 1. IPSdM were round or had an elongated shape with 2 or more processes (see arrows). Scale bar: 100 µm. **C.** Growth rate of four iPSdM lines. All iPSdM lines showed a similar growth behavior with a mean doubling time of 24.6 ± 1.1 h (iPSdM1), 26.3 ± 2.0 h (iPSdM2), 27.1 ± 1.4 h (iPSdM3) and 25.4 ± 1.4 h (iPSdM4). Data are presented as mean ± SEM of three independent experiments.

3.1.3 Protein expression profile of iPSdM

Flow cytometry analysis was performed to check for surface marker expression and to further confirm microglial identity. The expression profile is exemplarily shown in Fig. 3.4 for iPSdM1.

All iPSdM lines showed a similar expression of the analyzed markers. A strong expression of CD11b, CD11c, CD16/32, CD36, CD40, CD45, CD49d (integrin α4), CD86 (B7.2), CD206 (mannose receptor) and CX3CR1 (fractalkine receptor) could be detected by all iPSdM lines. While iPSdM line 1 to 3 showed a strong expression of CD11b, this surface marker was expressed lower by iPSdM4. CD29 (integrin β1), MHC class II protein and sialic acid binding Ig-like lectins-11 (Siglec-11) were weakly expressed by all four microglial lines. In contrast, the stem cell marker CD34 was not expressed in any iPSdM line indicating that the microglial lines showed no stem cell properties anymore. CD14, an associated co-receptor of the LPS receptor complex, was not expressed in unstimulated cells by iPSdM line 1 and 4 whereas it was slightly expressed by line 2 and 3. However, stimulation with LPS or IFNγ for 4 days increased the expression of CD14 (Fig. 3.4 B). Flow cytometry data indicate that the iPSdM lines express surface markers typical for microglia and that the expression of these markers remains stable up to passage 25 (data not shown).

Due to highly comparable results between the four iPSdM lines, in further experiments iPSdM1 has been used as a model line for the investigation of the functional characteristics.

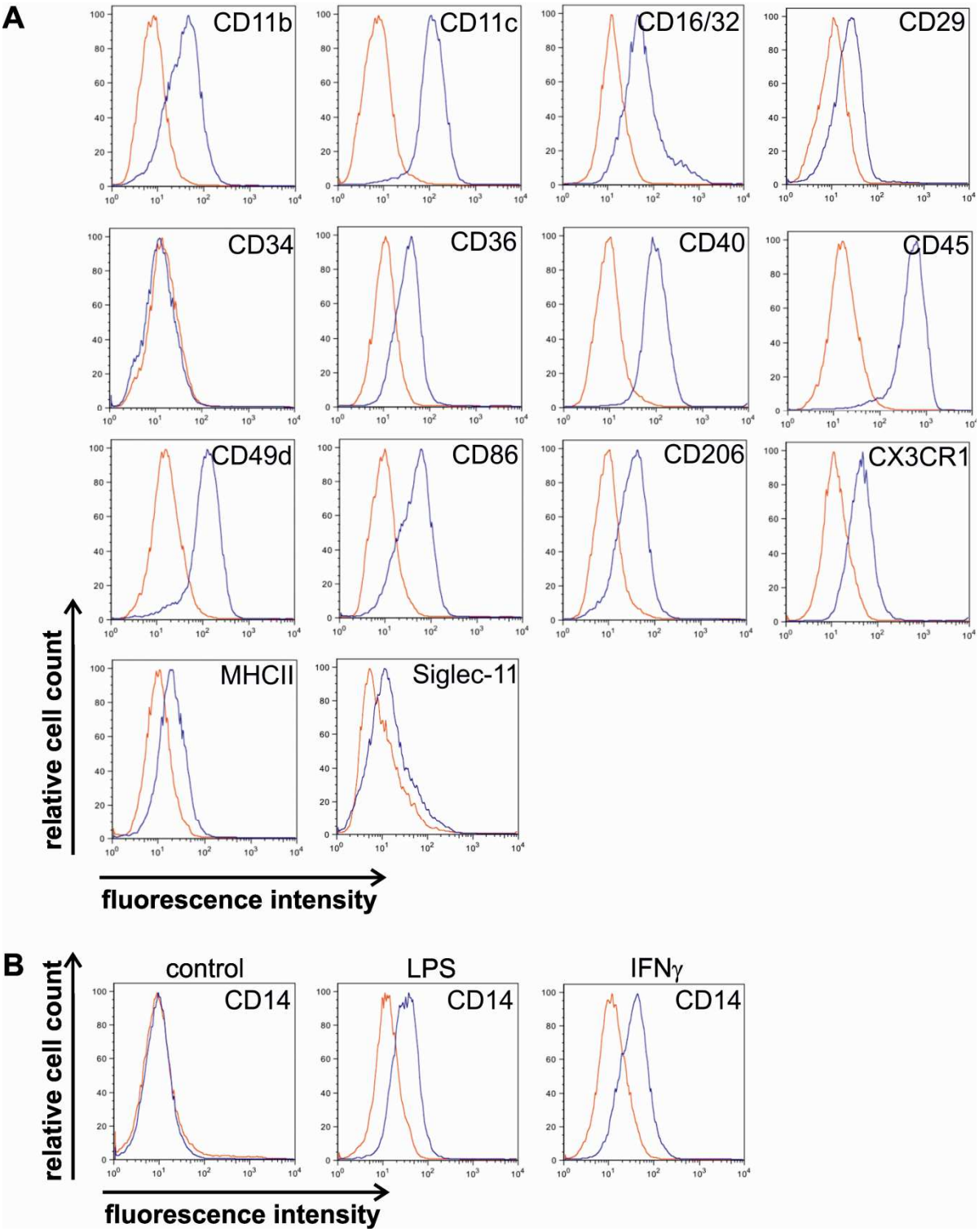

Fig. 3.4: Representative pictures of iPSdM1 surface marker expression. Representative pictures of flow cytometry analysis of iPSdM1. **A.** IPSdM1 showed expression of the microglial markers CD11b, CD11c, CD16/32, CD36, CD40, CD45, CD49d, CD86, CD206 and CX3CR1. Expression of CD29, MHC class II and Siglec-11 was very low on iPSdM1. The stem cell marker CD34 was not expressed. Signal from isotype control antibodies are shown in red, from surface markers are shown in blue. **B.** CD14 expression was not detected in unstimulated iPSdM1 while it was upregulated after stimulation for 96 h with LPS (1000 ng/ml) or IFNγ (1000 U/ml).

3.1.4 Relative cytokine gene transcription of iPSdM

One typical feature of microglia is the inducibility of pro-inflammatory cytokines after stimulation. Therefore, the transcript levels of TNFα and iNOS in iPSdM were analyzed using real-time RT-PCR (Fig. 3.5). Microglial precursors were stimulated with either LPS or IFNγ for 6 h. Unstimulated cells were used as control and set as 1. LPS and IFNγ stimulation had no impact on iNOS gene transcription (1.5 ± 0.4 fold and 1.2 ± 0.4 fold). In contrast, LPS stimulation significantly increased mRNA transcription of TNFα in iPSdM to 3.3 ± 0.5 fold ($p = 0.009$). However, IFNγ stimulation only led to a slight increase in gene transcription to 1.6 ± 0.4 fold. Data indicate that production of the pro-inflammatory cytokine TNFα could be significantly induced by LPS stimulation in iPSdM.

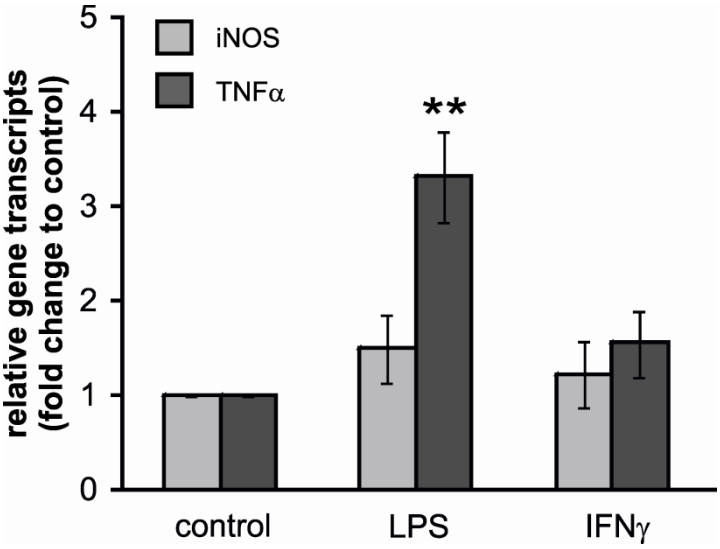

Fig. 3.5: Real-time RT-PCR analysis of iNOS and TNFα gene transcription by iPSdM1. IPSdM1 were unstimulated (control) or stimulated for 6 h with LPS (1000 ng/ml) or IFNγ (1000 U/ml). Both stimulations had no impact on iNOS gene transcription. Stimulation of iPSdM with LPS resulted in an increase of TNFα transcript levels, whereas IFNγ treatment did not alter the TNFα level. Values were normalized to GAPDH and control were set as 1. Data are presented as mean ± SEM of 6 independent experiments. ANOVA post-hoc Bonferroni p-values vs. control: ** $p \leq 0.01$.

3.1.5 Phagocytosis capacity of iPSdM

The phagocytosis capacity of microglia is an important functional hallmark. It has been shown that microglia are able to phagocytose amyloid β (Aβ) *in vitro*. The aggregation of Aβ is a pathological characteristic of Alzheimer's disease. Therefore, iPSdM were investigated regarding their phagocytosis capacity of Aβ and microsphere beads.

The phagocytosis assay with Aβ required the incubation of iPSdM with biotinylated Aβ. Microglial precursors were labelled with an antibody directed against Iba1. Using confocal microscopy and 3D reconstruction Aβ could be detected within the Iba1 positive microglial cells (Fig. 3.6 A). Quantification of Aβ positive cells revealed that 18.1 ± 3.3 % of the cells phagocytosed Aβ. To investigate the effect of a pro-inflammatory stimulation on phagocytosis behavior of microglial precursors, iPSdM were stimulated for 24 h with either LPS or IFNγ. Cells which have phagocytosed Aβ were counted and standardized to the total cell number (Fig. 3.6 B). LPS or IFNγ stimulated iPSdM were compared to unstimulated cells which were used as control and set as 100 %. Aβ phagocytosis was significantly increased to 196.6 ± 22.6 % ($p = 0.006$) after LPS stimulation and to 200.1 ± 21.2 % ($p = 0.005$) after IFNγ stimulation in comparison to the control (100.0 ± 17.3 %). Nearly no difference in phagocytosis capacity of Aβ could be observed between both stimulations. In summary, it could be determined that iPSdM took up Aβ and showed a significant increase in Aβ phagocytosis after stimulation with either LPS or IFNγ in comparison to the unstimulated control.

Additionally, the phagocytosis rate of iPSdM regarding microsphere beads was investigated. Microglial precursors were incubated with fluorescent labeled microsphere beads and analyzed using flow cytometry (Fig. 3.6 C). Cells without beads incubation served as negative control. The number of iPSdM phagocytosing more than 1 bead was calculated. In the unstimulated sample (control), 32.5 ± 5.7 % of the total cells showed beads uptake. Next, iPSdM were stimulated with either LPS or IFNγ for 24 h (Fig. 3.6 C+D) to detect whether pro-inflammatory stimulation would lead to an increased beads phagocytosis. Unstimulated cells were used as control and set as 100 %. LPS stimulation resulted in an increased uptake of microsphere beads to 128.5 ± 24.2 %. No effect of IFNγ stimulation on beads uptake could be observed (98.0 ± 16.8 %) in comparison to the unstimulated control (100.0 ± 17.3 %). In summary, iPSdM were able to

phagocytose microsphere beads, but uptake of beads could not be significantly increased with LPS or IFNγ treatment.

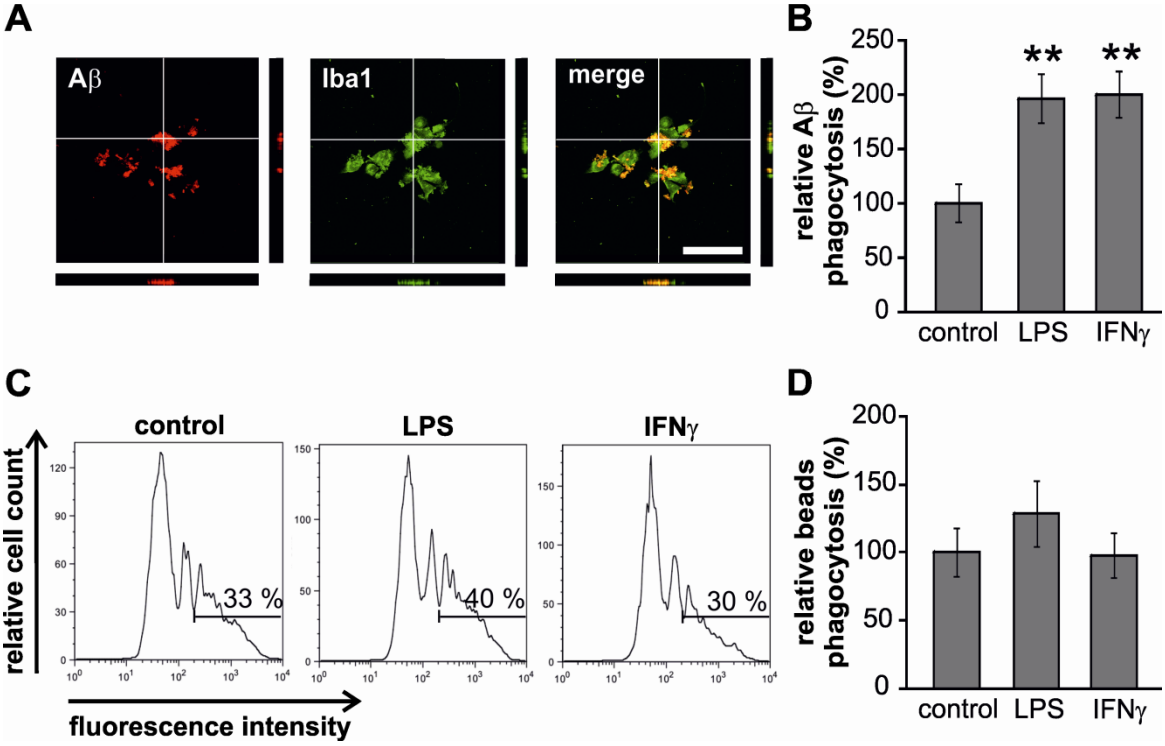

Fig. 3.6: Phagocytosis capacity of iPSdM1. A. Representative picture of Iba1 stained iPSdM1 phagocytosing amyloid β (Aβ). Biotinylated Aβ stained with Cy3 was detected inside the Iba1 positive microglial cells by confocal imaging and 3D reconstruction. **B.** Quantification of Aβ uptake by microglia. IPSdM1 were either untreated (control) or stimulated with 500 ng/ml LPS or 1000 U/ml IFNγ for 24 h. IPSdM1 showed an increased phagocytosis of fibrillary Aβ after stimulation with LPS or IFNγ. Data are presented as mean ± SEM of 4 independent experiments. ANOVA post-hoc Bonferroni p-values vs. control: ** $p \leq 0.01$. Ewgenija Gutjahr contributed to Fig. 3.5 B. **C.** Analysis of microsphere beads phagocytosis using flow cytometry. Cells were either untreated or stimulated with 500 ng/ml LPS or 1000 U/ml IFNγ for 24 h (from left to right). LPS stimulation increased beads uptake while IFNγ stimulation had no effect. **D.** Quantification of microsphere beads phagocytosis by iPSdM1. Cells were either unstimulated (control) or stimulated with 500 ng/ml LPS or 1000 U/ml IFNγ for 24 h. No significant difference in beads phagocytosis was observed between control and LPS or IFNγ stimulation. Data are presented as mean ± SEM of 5 independent experiments. ANOVA post-hoc Bonferroni p-values: n.s.

3.1.6 Migratory potential of iPSdM towards fractalkine

The fractalkine CX3CL1 is one of the major chemokines in the CNS and is mainly expressed by neurons. Microglia express the corresponding receptor CX3CR1. Using flow cytometry, the expression of the fractalkine receptor CX3CR1 by iPSdM was confirmed (Fig. 3.4). Now, the migration of iPSdM towards the fractalkine was investigated using a transwell-system (Fig. 3.7).

IPSdM were attracted through different concentrations of CX3CL1 (5, 10, 15 and 20 ng/ml). As control, 20 ng/ml of CX3CL1 were added to both the lower and the upper chamber of the transwell system to exclude undirected migration. Cells that had migrated to the lower chamber and to the backside of the membrane were counted and normalized to the migration without CX3CL1 (0 ng/ml) application (Fig. 3.7). The application of 5 ng/ml fractalkine resulted in a slight increase of migrated cells to 16.6 ± 2.3 % in comparison to the control (9.4 ± 1.9 %). The usage of 10 ng/ml fractalkine significantly increased the number of migrated cells to 28.4 ± 3.4 % ($p = 0.020$). Treatment with 15 ng/ml CX3CL1 significantly increased the number of migrated cells to 36.4 ± 2.6 % ($p = 0.001$) and 20 ng/ml CX3CL1 to 29.9 ± 6.0 % ($p = 0.011$). Interestingly, the fractalkine concentration of 20 ng/ml did not further increase the number of migrated cells in comparison to 15 ng/ml CX3CL1. In summary, a dose-dependent migration of iPSdM towards the fractalkine could be observed.

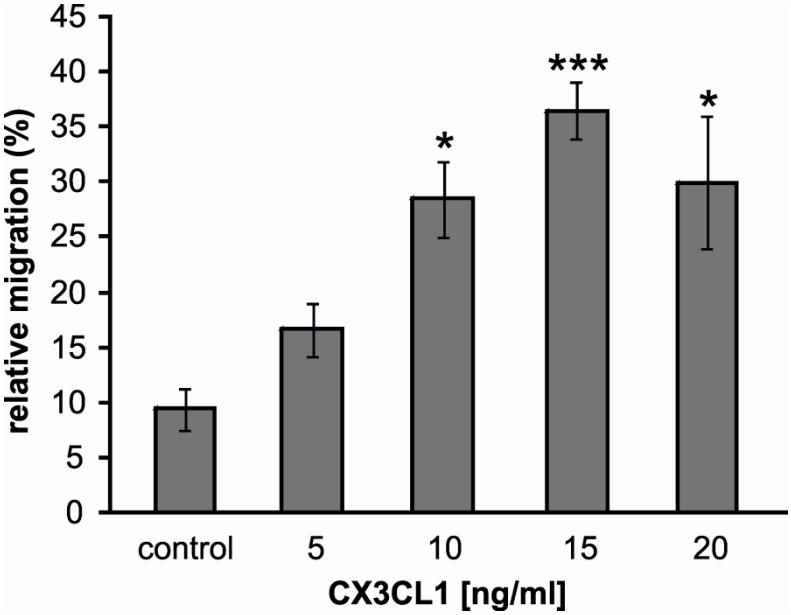

Fig. 3.7: *In vitro* transwell migration assay of iPSdM1 towards CX3CL1. Microglial precursor cells migrated in a dose-dependent manner towards the chemokine CX3CL1. To exclude undirected migration, 20 ng/ml CX3CL1 were added to both wells of the transwell system as control. Data are presented as mean ± SEM of 3 independent experiments. ANOVA post-hoc Bonferroni p-values vs. control: * $p \leq 0.05$, *** $p \leq 0.001$. Data obtained in cooperation with Ewgenija Gutjahr.

3.1.7 Engraftment of iPSdM into the CNS of immunodeficient mice

To study the engraftment into the CNS, iPSdM were lentivirally transduced with GFP. GFP expressing iPSdM were transplanted into the hippocampus (Fig. 3.8 A) of Rag2/IL-2R knockout mice lacking B cells, T cells and natural killer cells. Three and nine weeks post-transplantation mice were sacrificed, brains were isolated and 20 µm cryosections were prepared. Immunohistochemical analysis showed that GFP positive cells were detectable in the brain close to the injection area. Those GFP positive cells could be stained for the microglial marker CD68 indicating the microglial phenotype (Fig. 3.8 C). Moreover, GFP-iPSdM were localized next to GFAP positive astrocytes. Furthermore, GFP-iPSdM integrated into the brain tissue, migrated out of the dentate gyrus and built processes (Fig. 3.8 B). The number of GFP-iPSdM integrated into the brain tissue was analyzed three and nine weeks post-transplantation (Fig. 3.8 D). After three weeks 48.4 ± 8.9 cells/mm² and after nine weeks 26.7 ± 11.3 cells/mm² were found in the dentate gyrus. Cells were distributed over an area of 0.4 ± 0.1 mm² (3 weeks) and 0.7 ± 0.1 mm² (9 weeks). Next, the number of GFP positive cells migrated out of

the dentate gyrus was counted. After 3 weeks 6.3 ± 2.5 % and after nine weeks 56.3 ± 4.5 % of GFP-iPSdM migrated out of the dentate gyrus. In summary, GFP-iPSdM could be transplanted into the brain of immunodeficient mice where they migrated and integrated into the brain tissue.

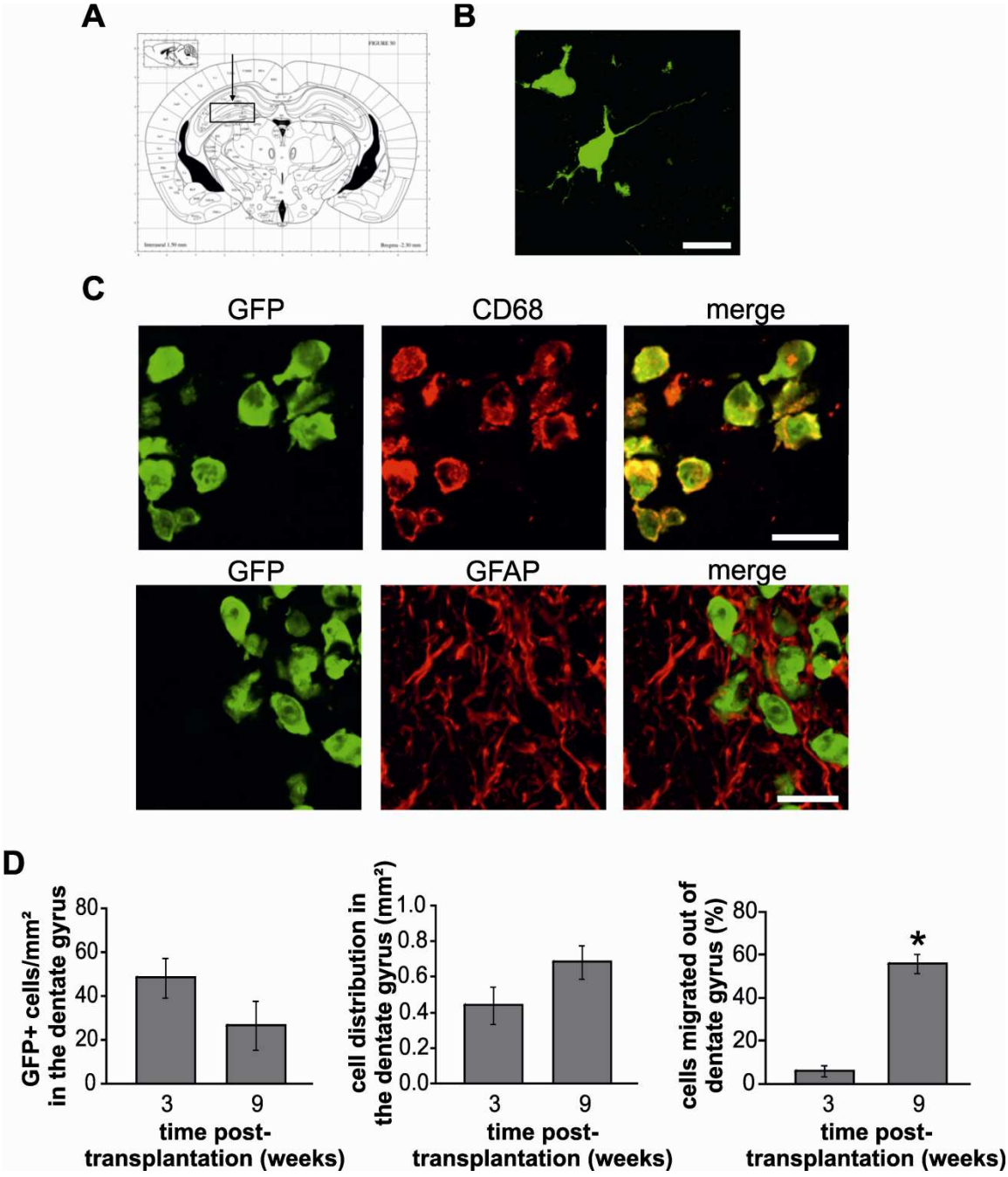

Fig. 3.8: Engraftment of GFP transduced iPSdM1 into the CNS of immunodeficient mice. IPSdM1 were lentivirally transduced with GFP and transplanted into the hippocampus of immunocompromised Rag2/IL-2R deficient mice. **A.** Schematical illustration of a frontal mouse brain section taken from the mouse brain atlas of Paxinos and Franklin, which shows the transplantation area (referred to Bregma: 2.4/1.5/1.4-1.6) of GFP-iPSdM1 into Rag2/IL-2R deficient mice. **B.** Nine weeks post-transplantation mice were sacrificed and cortical tissue sections were

analyzed for GFP positive cells. GFP-iPSdM integrated into the brain tissue and buil processes. Scale bar: 25 µm. **C.** Nine weeks post-transplantation mice were sacrificed and cortical tissue sections were immunostained with antibodies directed against the microglial marker CD68 and the astrocytic marker GFAP. GFP-iPSdM1 engrafted into the brain tissue, were stained for CD68 and localized nearby GFAP positive astrocytes. Scale bars: 25 µm. **D.** Quantification of transplanted GFP-iPSdM1 in the dentate gyrus of Rag2/IL-2R deficient mice 3 and 9 weeks post-transplantation. No significant difference in GFP positive cells /mm² as well as their distribution in the dentate gyrus was observed. However, 9 weeks post-transplantation more cells migrated out of the dentate gyrus in comparison to 3 weeks post-transplantation. Data are presented as mean ± SEM. Student's t-test p-values: * $p \leq 0.05$.

3.2 iPSdM as a model system for SOD1 mediated amyotrophic lateral sclerosis

ALS is a neurodegenerative disease characterized by progressive muscle weakness, inflammation and microglial activation. In familial ALS, the most common causes are mutations in the SOD1 gene. This protein catalyzes the conversion of superoxide to hydrogen peroxide. The expression of mSOD1 in neurons leads to motor neuron degeneration. Accumulation of mSOD1 in microglia does not affect disease onset but the progression of the disease. However, the role of mSOD1 in microglia is not fully understood so far. Thus, mSOD1 in microglia might have a critical role in exacerbating the disease. However, the exact mechanism involved is still unclear.

3.2.1 Transduction of iPSdM with mutant SOD1

In order to study the role of mSOD1 in human microglia, iPSdM1 were transduced with human mSOD1. Three different mutations of SOD1 involved in ALS pathology were used: GFP-tagged human SOD1-G37R, -G85R and -G93A. GFP alone and wildtype (wt) SOD1 transduced cells served as controls. To verify the expression of SOD1, cells were stained with antibodies directed against SOD1. Using confocal images and 3D reconstruction SOD1 could be detected inside the GFP positive cells throughout the cytoplasm (Fig. 3.9).

Furthermore, a western blot was carried out to elucidate the expression level of mSOD1 in comparison to endogenous SOD1 (Fig. 3.10 A). Endogenous SOD1 was present in all cell lysates. SOD1-GFP (mSOD1) was detected in iPSdM transduced with wt or mutant SOD1 and absent in GFP-iPSdM. The ratio of mSOD1 to endogenous SOD1 was calculated (Fig. 3.10 B). Ratio was 4.9 ± 0.8 fold for iPSdM-SOD1 wt, 11.7 ± 5.9 fold for -SOD1 G37R, 3.9 ± 2.1 fold for -SOD1 G85R and 1.6 ± 0.1 fold for -SOD1 G93A.

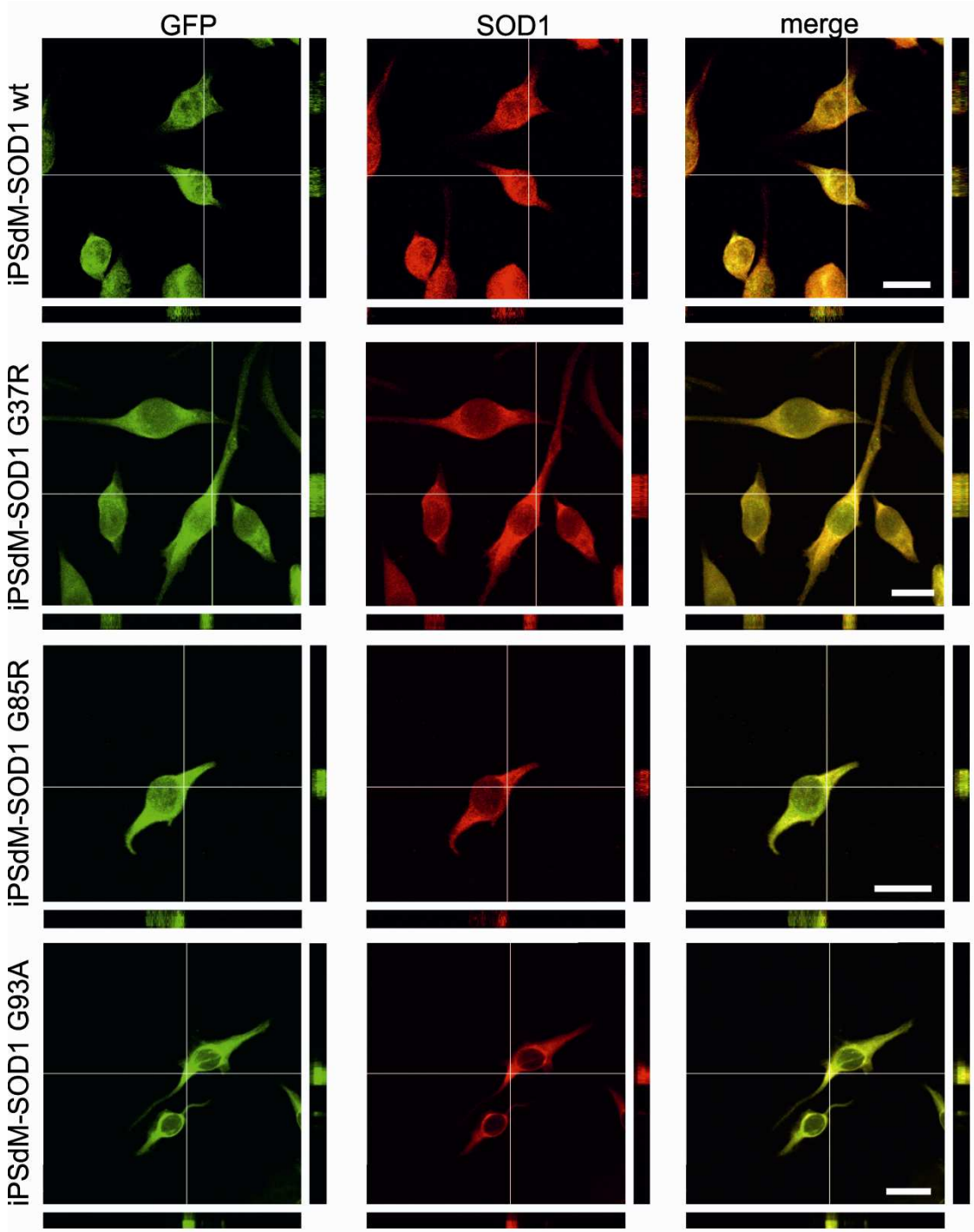

Fig. 3.9: Expression of wildtype and human mutant SOD1 by iPSdM1 detected via immunocytochemistry. IPSdM1 were lentivirally transduced with wildtype (wt) or three different mutants of GFP-tagged human SOD1 (SOD1 G37R, G85R and G93A). GFP-positive iPSdM1 were stained with an antibody directed against SOD1. SOD1 was detected inside GFP-positive cells using confocal microscopy and 3D reconstruction. Scale bars: 20 µm.

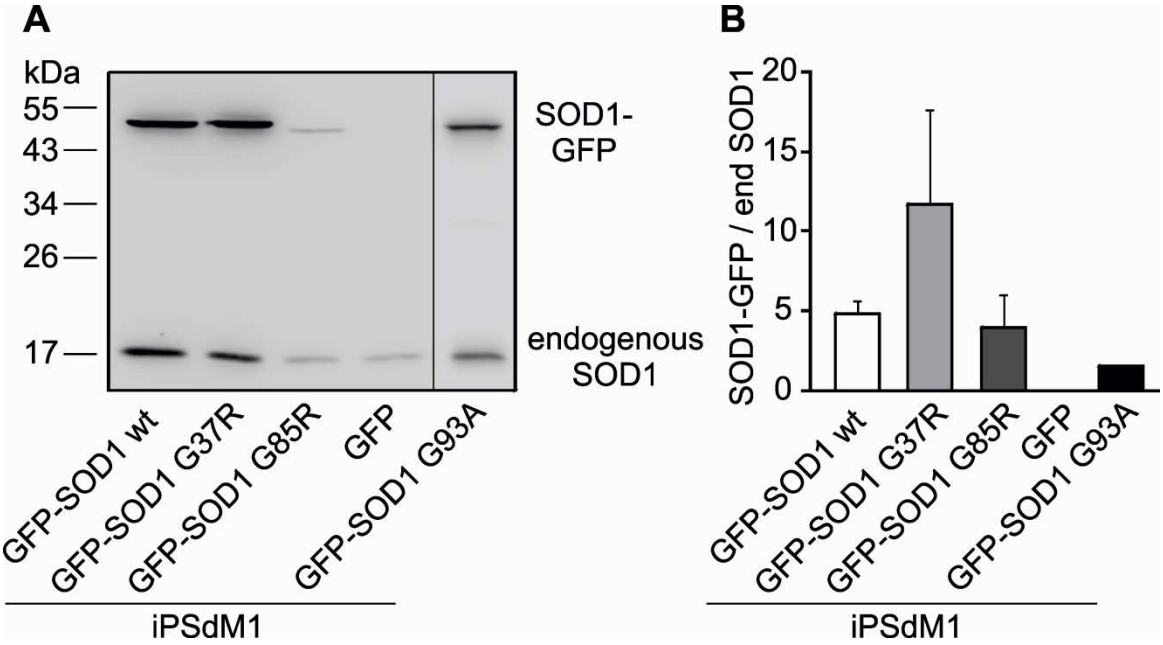

Fig. 3.10: Western blot analysis of the expression of wildtype and human mutant SOD1 by iPSdM1. IPSdM1 were lentivirally transduced with wildtype (wt) or three different mutants of GFP-tagged human SOD1 (SOD1 G37R, G85R and G93A). **A.** Western Blot analysis of endogenous SOD1 (19 kDa) and SOD1-GFP (mSOD1) (50 kDa) which were detected by an HRP-coupled secondary antibody in wt and mSOD1 expressing cells. GFP-iPSdM1 were used as control and showed a slight band for endogenous SOD1 but no band for GFP-SOD1. Representative western blot out of 3 independent experiments. **B.** Ratio of expressed SOD1-GFP (mSOD1) to endogenous SOD1 in wt and mSOD1 expressing iPSdM1. Ratio was 4.9 ± 0.8 fold for iPSdM-SOD1 wt, 11.7 ± 5.9 fold for -SOD1 G37R, 3.9 ± 2.1 fold for -SOD1 G85R and 1.6 ± 0.1 fold for -SOD1 G93A. GFP-iPSdM did not express SOD1-GFP. Data are presented as mean + SEM of 3 independent experiments. Data were obtained in cooperation with Dr. Clement, University of Mainz.

3.2.2 Viability and proliferation of mutant SOD1 expressing iPSdM

Using MTT assay, cell viability of iPSdM expressing GFP, wt or mSOD1 was investigated (Fig. 3.11 A). The relative cell viability was normalized to non-transduced iPSdM which were set as 100 %. No significant difference in cell viability was observed between GFP-iPSdM (84.63 ± 2.31 %), iPSdM-SOD1 wt (105.49 ± 5.39 %), -SOD1 G37R (97.33 ± 7.24 %), -SOD1 G85R (89.88 ± 5.37 %) and -SOD1 G93A (97.93 ± 13.29 %).

To determine a possible difference in the growth rates between the mSOD1 expressing iPSdM lines a proliferation assay was performed (Fig. 3.11 B). A defined cell number was seeded and cells were counted every 24 h for a total of 96 h. The mSOD1 expressing iPSdM showed a similar growth behavior among each other and in comparison to GFP-iPSdM and non-transduced iPSdM. Non-

transduced iPSdM had a mean doubling time of 24.6 ± 1.1 h (Fig. 3.3 C). GFP-iPSdM showed a mean doubling time of 25.2 ± 1.5 h, iPSdM-SOD1 wt of 25.1 ± 2.5 h, -SOD1 G37R of 24.9 ± 5.2 h, -SOD1 G85R of 24.2 ± 2.2 h and -SOD1 G93A of 26.8 ± 2.0 h.

In summary, transduction of iPSdM with GFP or different mSOD1 changed neither cell viability nor growth behavior in comparison to non-transduced cells.

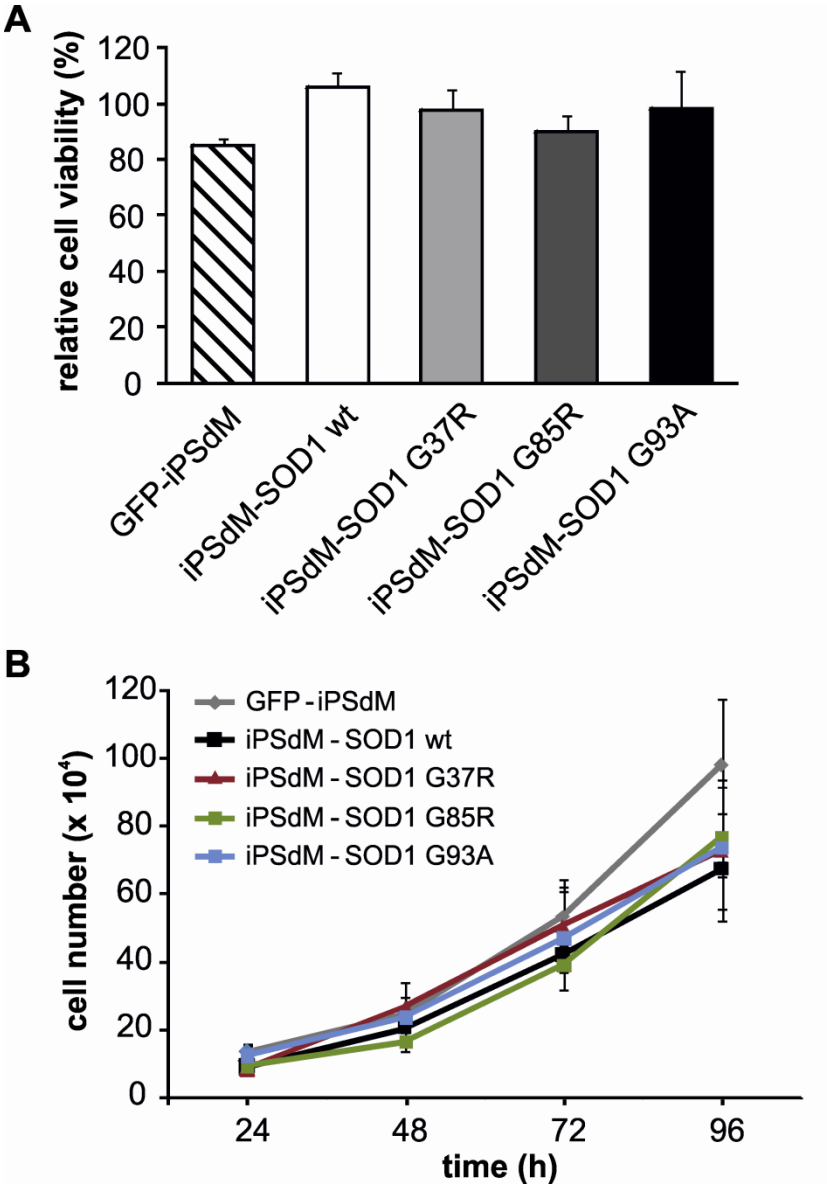

Fig. 3.11: Cell viability and growth rate of iPSdM1 expressing GFP, wt or mutant SOD1. IPSdM1 were lentivirally transduced with wildtype (wt) or different mSOD1. **A.** Cell viability assay of GFP, wt and mSOD1 expressing iPSdM1. Cell viability of mSOD1 expressing iPSdM was detected with a MTT assay and compared to iPSdM1 set as 100 %. GFP, wt and mSOD1 expressing iPSdM1 showed no difference in cell viability compared to iPSdM. Data are presented as mean + SEM of 3 independent experiments. ANOVA post-hoc Bonferroni p-values vs. iPSdM1: n.s. **B.** Growth rate of GFP, wt and mSOD1 expressing iPSdM1. All lines showed a similar growth rate

with a mean doubling time of 25.2 ± 1.5 h for GFP-iPSdM, 25.1 ± 2.5 h for iPSdM-SOD1 wt, 24.9 ± 5.2 h -SOD1 G37R, 24.2 ± 2.2 h for -SOD1 G85R and 26.8 ± 2.0 h for -SOD1 G93A. Data are presented as mean ± SEM of 3 independent experiments.

3.2.2 TNFα transcript levels of mutant SOD1 expressing iPSdM

Microglia might act neurotoxic through the release of pro-inflammatory cytokines. The expression of mSOD1 by microglia could influence the production of pro-inflammatory cytokines. Therefore, GFP, wt or mSOD1 expressing iPSdM were stimulated with LPS, IFNγ or TNFα for 6 h and inducibility of TNFα transcription was analyzed via real-time RT-PCR (Fig. 3.12). Untreated cells served as control and were set as 1.

LPS stimulation increased TNFα transcription to 4.7 ± 1.0 fold (p=0.021) in GFP-iPSdM, 3.0 ± 0.9 fold in iPSdM-SOD1 wt, 4.3 ± 1.5 fold in -SOD1 G37R, 2.8 ± 0.1 fold (p=0.000) in -SOD1 G85R and 7.4 ± 5.1 fold in -SOD1 G93A.

IFNγ and TNFα stimulation had no effect on TNFα transcription. IFNγ stimulation led to a TNFα transcription of 1.0 ± 0.1 fold in GFP-iPSdM, 1.4 ± 0.2 fold in iPSdM-SOD1 wt, 1.4 ± 0.4 fold in -SOD1 G37R, 1.1 ± 0.2 fold in -SOD1 G85R and 1.8 ± 0.7 fold in -SOD1 G93A. TNFα stimulation led to a TNFα transcription of 1.6 ± 0.8 fold in GFP-iPSdM, 1.1 ± 0.2 fold in iPSdM-SOD1 wt, 1.2 ± 0.4 fold in -SOD1 G37R, 0.8 ± 0.1 fold in -SOD1 G85R and 1.1 ± 0.3 fold in -SOD1 G93A.

No difference in TNFα transcription was observed between GFP-iPSdM and iPSdM-SOD1 wt cells. TNFα transcription was not significantly different between wt or mSOD1 expressing iPSdM.

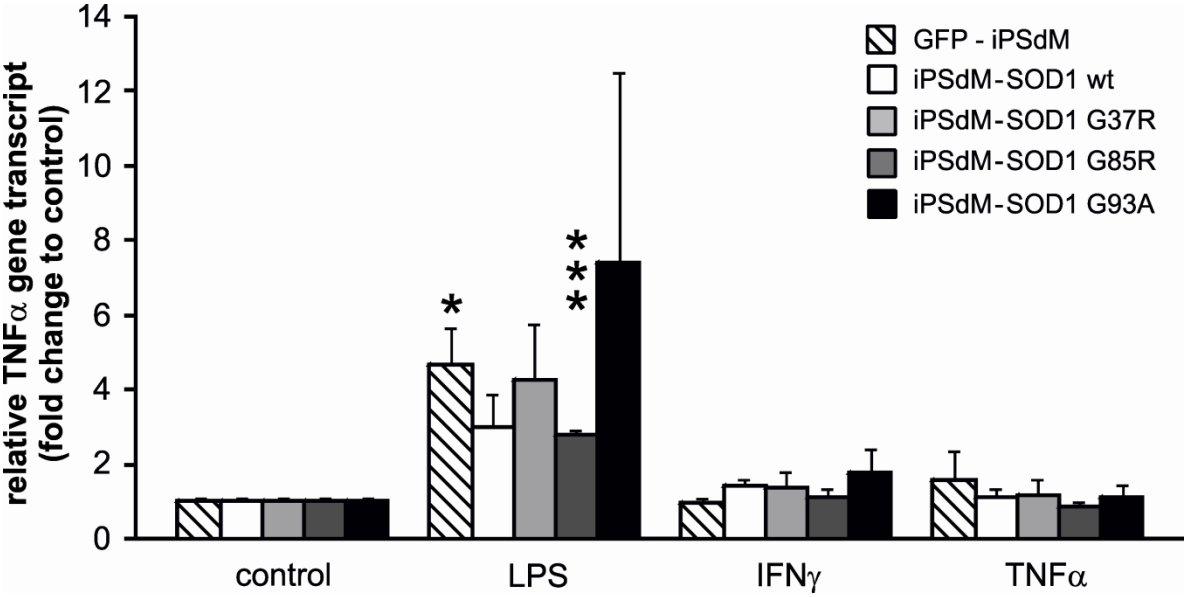

Fig. 3.12: TNFα gene transcript analysis of iPSdM1 expressing GFP, wt or mutant SOD1. TNFα gene transcripts of wt and mSOD1 expressing iPSdM1 lines were analyzed using real-time RT-PCR. Cells were either unstimulated (control) or treated with 1000 ng/ml LPS, 1000 U/ml IFNγ or 100 ng/ml TNFα for 6 h. No significant differences in the gene transcription of TNFα were observed between the GFP-iPSdM and iPSdM expressing SOD1 wt or mutant SOD1. Data are presented as mean + SEM of 3 independent experiments. ANOVA post-hoc Bonferroni p-values vs. control: * $p \leq 0.05$, *** $p \leq 0.001$.

3.2.3 Mitochondrial analysis of mutant SOD1 expressing iPSdM

In mSOD1 expressing cells, the morphology and function of mitochondria can be impaired. In this study, mitochondrial activity of complex I (NADH:ubichinone reductase), complex IV (cytochrome c oxidase) and citrate synthase were investigated (Fig. 3.13).

No difference in the activity of complex I, complex IV or citrate synthase was detected in unstimulated cells. Activities for complex I were 0.016 ± 0.002 U/mg for GFP-iPSdM, 0.016 ± 0.004 U/mg for iPSdM-SOD1 wt, 0.019 ± 0.002 U/mg for -SOD1 G37R, 0.014 ± 0.002 U/mg for -SOD1 G85R and 0.019 ± 0.003 U/mg for -SOD1 G93A expressing iPSdM. Activities for complex IV were 0.356 ± 0.124 U/mg for GFP-iPSdM, 0.459 ± 0.124 U/mg for iPSdM-SOD1 wt, 0.525 ± 0.059 U/mg for -SOD1 G37R, 0.467 ± 0.196 U/mg for -SOD1 G85R and 0.362 ± 0.024 U/mg for -SOD1 G93A expressing iPSdM. Citrate synthase activities were 0.410 ± 0.005 U/mg for GFP-iPSdM, 0.385 ± 0.034 U/mg for iPSdM-SOD1 wt, 0.382 ± 0.013 U/mg for -SOD1 G37R, 0.360 ± 0.006 U/mg for -SOD1 G85R and 0.472 ± 0.101 U/mg for -SOD1 G93A expressing iPSdM.

Furthermore, activities of complex I, complex IV and citrate synthase were measured in cells stimulated for 24 h with LPS, IFNγ or TNFα. However, no differences in enzyme activities for all enzymes were measured for any stimulation in comparison to unstimulated cells or in among the different cell lines (data not shown).

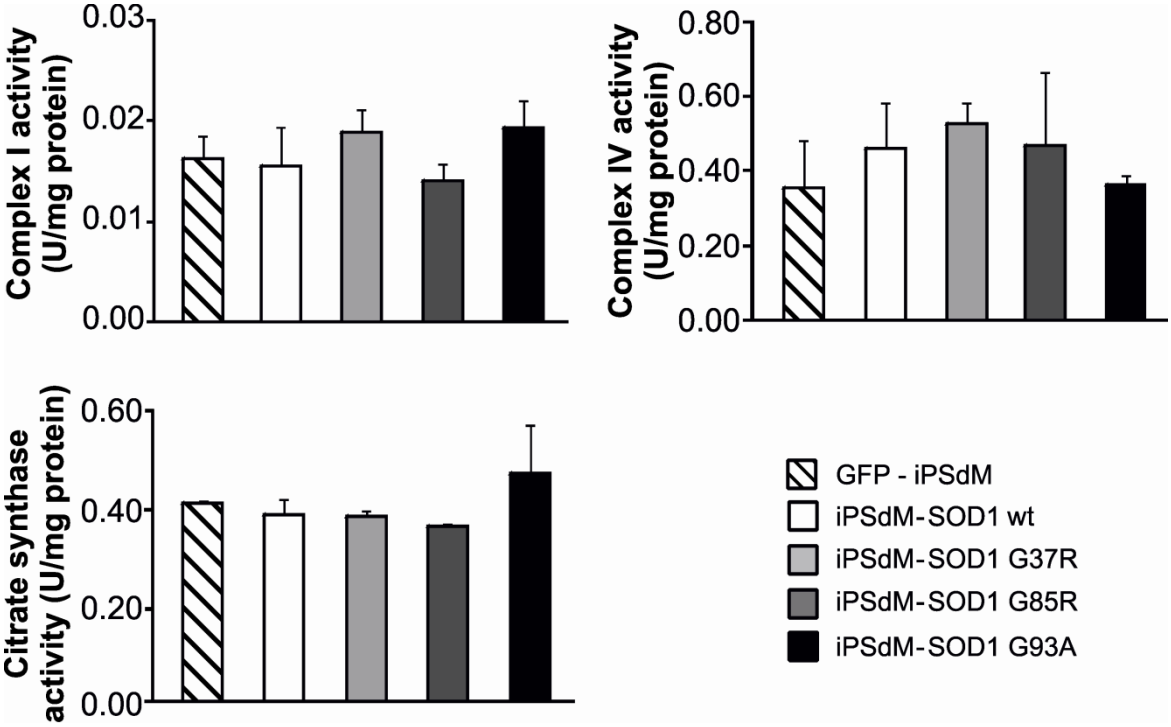

Fig. 3.13: Mitochondrial analysis of iPSdM1 expressing GFP, wt or mutant SOD1. Protein lysates of iPSdM1 genetically modified with the genes for GFP, SOD1 wt, SOD1 G37R, SOD1 G85R and SOD1 G93A were analyzed for activity of the mitochondrial respiratory chain enzymes complex I, complex IV and citrate synthase. No differences in enzyme activities were observed between the iPSdM1 lines expressing GFP, SOD1 wt, SOD1 G37R, SOD1 G85R or SOD1 G93A. Data are presented as mean + SEM of 3 independent experiments. ANOVA post-hoc Bonferroni p-values: n.s. Data were obtained in cooperation with Prof. Kunz, University of Bonn.

3.2.4 Production of ROS by mutant SOD1 expressing iPSdM

SOD1 is responsible for the conversion of superoxide to hydrogen peroxide. Mutation of SOD1 might lead to an increase in the production and release of ROS. Therefore, ROS production of mSOD1 expressing iPSdM in comparison to SOD1 wt and GFP expressing iPSdM was investigated.

Dihydroethidium (DHE) reacts with superoxide leading to a bright red colour inside the cells depending on the amount of ROS. DHE staining of unstimulated cells showed nearly no difference among all lines (Fig. 3.14 A). Stimulation with TNFα

for 20 min increased DHE intensity of iPSdM-SOD1 G37R, -SOD1 G85R and -SOD1 G93A but not for GFP-iPSdM or iPSdM-SOD1 wt (Fig. 3.14 A).

Using confocal imaging, DHE intensity was quantified and normalized to unstimulated control cells which were set as 1 (Fig. 3.14 B). TNFα stimulation did not alter the relative DHE intensity in GFP-iPSdM (1.20 ± 0.18 fold) and in iPSdM-SOD1 wt (1.05 ± 0.06 fold). In contrast, relative DHE intensity of iPSdM-SOD1 G37R was significantly increased to 2.30 ± 0.46 fold in comparison to the control ($^{+}$ p=0.006) and to SOD1 wt expressing iPSdM (* p=0.037). In comparison to the control, relative DHE intensity was significantly increased to 2.10 ± 0.33 fold ($^{+}$ p=0.000) in iPSdM-SOD1 G85R and to 1.77 ± 0.25 fold ($^{+}$ p=0.007) in iPSdM-SOD1 G93A. However, no significant difference in DHE intensity of SOD1-G85R and -G93A expressing iPSdM in comparison to wt cells was observed after TNFα stimulation.

Next, cells were stimulated with LPS or IFNγ for 24 h and DHE intensity was quantified to the control cells which were set as 1 (Fig. 3.14 C). LPS stimulation did not lead to a difference in relative DHE intensity between GFP-iPSdM (0.87 ± 0.11 fold), iPSdM-SOD1 wt (1.02 ± 0.08 fold) and -SOD1 G37R (0.98 ± 0.09 fold). Relative DHE intensity was increased in iPSdM-SOD1 G85R to 1.37 ± 0.14 fold. LPS stimulation led to a significant increase in relative DHE intensity in iPSdM-SOD1 G93A to 1.51 ± 0.16 fold (* p=0.037) in comparison to wt cells.

IFNγ stimulation did not alter relative DHE intensity of GFP-iPSdM (1.60 ± 0.35), iPSdM-SOD1 wt (1.26 ± 0.08 fold), -SOD1 G37R (1.32 ± 0.27 fold) and -SOD1 G85R (1.33 ± 0.10 fold). However, IFNγ stimulation led to a significant increase in iPSdM-SOD1 G93A to 2.29 ± 0.27 fold in comparison to the control ($^{+}$ p=0.000) and to SOD1 wt cells (* p=0.007).

In summary, in comparison to wt cells DHE intensity was significantly increased in iPSdM-SOD1 G37R after TNFα stimulation whereas iPSdM-SOD1 G93A react to LPS and IFNγ stimulation.

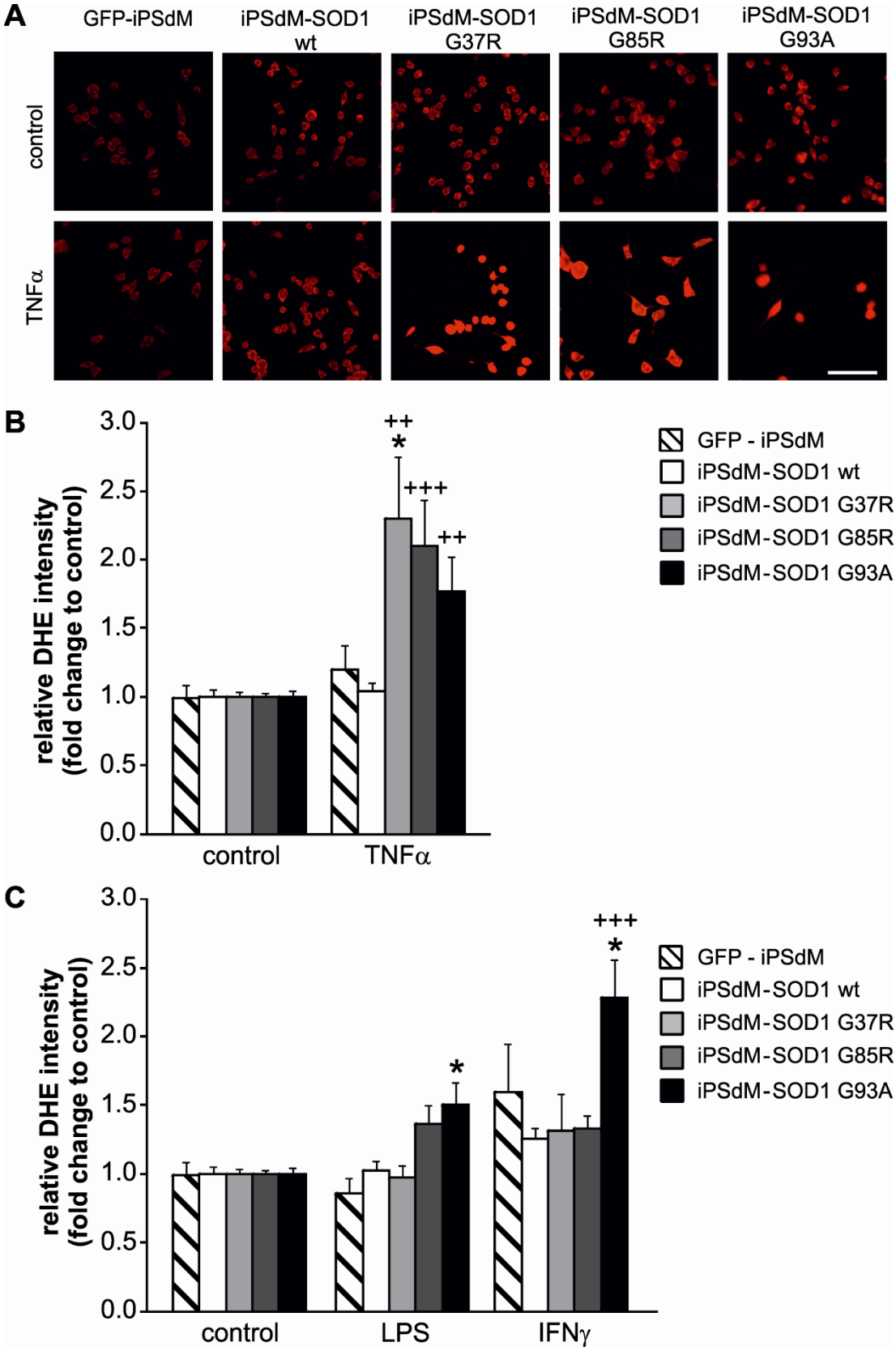

Fig 3.14: Reactive oxygen species production by iPSdM1 expressing GFP, wt or mutant SOD1. A. Confocal images for detection of reactive oxygen species (ROS) by DHE staining. IPSdM1 expressing GFP, wt or mSOD1 were unstimulated (control) or stimulated with 500 ng/ml TNFα for 20 min and ROS production was analyzed via DHE staining and confocal images.

IPSdM1 expressing SOD1 G37R, SOD1 G85R and SOD1 G93A showed an increased DHE signal after TNFα stimulation in comparison to GFP-iPSdM and iPSdM-SOD1 wt. Scale bar: 100 µm. **B+C.** Quantification of DHE intensity after TNFα (B), LPS or IFNγ (C) stimulation. IPSdM1 expressing GFP, wt or mSOD1 were either untreated (control) or stimulated with 500 ng/ml TNFα for 20 min (B), 1000 ng/ml LPS or 1000 U/ml IFNγ for 24 h (C). GFP-iPSdM showed no difference in DHE intensity in comparison to SOD1 wt expressing iPSdM. IPSdM1 expressing SOD1 G37R, SOD1 G85R and SOD1 G93A showed an increased DHE signal after TNFα stimulation in comparison to iPSdM-SOD1 wt and GFP-iPSdM. IPSdM1 expressing SOD1 G93A showed a significant increased DHE signal after LPS or IFNγ stimulation in comparison to iPSdM-SOD1 wt. Data are presented as mean + SEM of 3 independent experiments. ANOVA post-hoc Bonferroni p-values vs. corresponding stimulation of iPSdM-SOD1 wt: * $p \leq 0.05$ or vs. control of the same cell line: ++ $p \leq 0.01$, +++ $p \leq 0.001$.

3.3 Summary

The aim of this work was to establish microglial precursor lines derived from human induced pluripotent stem cells. In total, four different microglial precursor lines (iPSdM) out of 2 different donors have been obtained. Analysis of different microglial markers confirmed a strong expression of CD11b, CD11c, CD16/32, CD36, CD40, CD45, CD49d, CD86, CD206 and CX3CR1, while expression of the stem cell marker CD34 was absent. IPSdM showed characteristic hallmarks of microglia such as the inducibility of pro-inflammatory cytokines, phagocytosis and migratory capacity. In detail, pro-inflammatory cytokine production of TNFα was induced after LPS stimulation. Furthermore, iPSdM phagocytosed Aβ and microsphere beads. A dose-dependent migration towards the fractalkine CX3CL1 by iPSdM was observed. Moreover, iPSdM could be transplanted into the hippocampus of immunodeficient mice where they migrated and integrated into the brain tissue. Thus, iPSdM showed characteristics of primary microglia.

Next, iPSdM were used as a model for SOD1-mediated ALS. IPSdM were lentivirally transduced to overexpress wt or three different SOD1 mutations (G37R, G85R and G93A) and were then investigated. No differences in proliferation and cell viability were observed between wt and the different mSOD1 expressing iPSdM. LPS, IFNγ or TNFα stimulation did not lead to a significant difference in the production of TNFα between SOD1 wt and mSOD1 expressing iPSdM. Furthermore, no differences in the activities of the mitochondrial enzymes complex I, complex IV and citrate synthase were observed between wt and mSOD1-iPSdM. However, ROS production was increased after TNFα stimulation in SOD1 G37R and after LPS and IFNγ stimulation in SOD1 G93A expressing iPSdM in comparison to iPSdM-SOD1 wt.

5 Discussion

The CNS is regarded as an immune privileged organ as it is shielded around the periphery by the blood-brain barrier and the blood-cerebrospinal-barrier. Thereby, unlimited entry of blood-derived leukocytes into the CNS can be prevented (Streit, 2002). Microglia are the only mononuclear phagocytes which represent the immune system of the CNS (Ransohoff and Cardona, 2010). Microglia are distributed throughout the whole brain and monitor their microenvironment. Upon stimuli microglia become activated, migrate to the site of stimuli, clear debris and apoptotic cells, promote tissue repair and release soluble neurotrophic factors (Streit, 2002; Block *et al.*, 2007). However, pro-inflammatory activated microglia can also be neurodestructive through the release of toxic factors like reactive oxygen species. It is also reported that microglia are involved in the pathogenesis of neurodegenerative diseases (Block and Hong, 2005). Therefore, detailed studies about microglial function in the healthy and diseased brain are crucial.

Primary microglia derived from brains of postnatal mice or rats are often used to study microglial function. Primary cells can be obtained by a shaking procedure of mixed glial cells (Giulian and Baker,1986). Alternatively, a purified population of microglial cells can be obtained using density gradients and flow cytometric sorting (Ford *et al.*, 1995). Human microglia can only be obtained in very limited numbers from patients undergoing neurosurgery or from post-mortem brains. Recently, a new protocol for human microglial isolation was developed (Olah *et al.*, 2011). The protocol requires the mechanical dissociation of the brain and density gradient purification providing high purity microglia populations. However, the marginal availability of human primary microglia complicates biological and functional analysis.

Two different microglial cell lines were developed. One from embryonic brain-derived macrophages (Janabi *et al.*, 1995) and the other from microglia isolated from primary cultures of embryonic human telencephalon (Nagai *et al.*, 2001). However, due to the transformation process these cell lines might have an altered cytokine profile and are not suitable for therapeutic approaches. Therefore, oncogenically transformed cells might not reflect microglial behavior appropriately.

In this work, microglial precursors were differentiated from human iPS cells to overcome the limitations of insufficient cell numbers and alterations due to transduction processes. The generated iPSdM were highly proliferative and could be cultivated for 25 passages without losing their properties. Furthermore, the differentiation protocol allows the generation of microglial precursors from iPS cells derived from patients with neurodegenerative disorders. Thus, this method provides the possibility to study microglial characteristics and function in human neurodegenerative diseases.

4.1 Generation and characterization of iPSdM

4.1.1 Generation of iPSdM

The differentiation procedure was based on a five-step-protocol recently developed in our laboratory to generate microglial precursors (ESdM) from mouse embryonic stem cells (Napoli *et al.*, 2009; Beutner *et al.*,2010). Differentiation required EB formation followed by neural induction. The protocol is derived from a neuroectodermal differentiation protocol leading to the co-development of neurons and astrocytes along with microglial precursors. This protocol is based on the observation that embryonic stem cell differentiation in culture comprises haematopoiesis as found in the yolk sac which give rise to primitive nucleated erythroid cells and macrophages (Keller *et al.*, 1993; Inamdar *et al.*, 1997).

The origin of microglia was under debate for decades including hypotheses from mesodermal to neuroectodermal origin (Chan *et al.*, 2007; Takashima *et al.*, 2007). Fate mapping analysis in mice revealed that embryonic macrophages from the yolk sac give rise to microglia (Ginhoux *et al.*, 2010; Ransohoff and Cardona, 2010). Nearly all adult microglia seemed to arise from these macrophages around embryonic day 7.5.

Therefore, the ESdM develop from a yolk sac intermediate stage and moreover get environmental signals from developing neurons and astrocytes. In respect to their cell surface markers, ESdM are identical to primitive macrophages derived from the yolk sac (Bertrand *et al.*, 2005; Napoli *et al.*, 2009; Beutner *et al.*, 2010).

A similar developmental program of human microglia can be suggested. Differentiation of human embryonic stem cells to EBs models earliest events of embryonic hematopoiesis demonstrating yolk sac development and generation of

immature CD45 positive macrophages (Zambidis *et al.*, 2005). Therefore, it can be presumed that human microglia develop from macrophages in the yolk sac as well.

In this work, two different iPS cell lines from healthy individuals were used to generate four microglial precursor lines. Human fibroblasts were reprogrammed to iPS cells using a retroviral system with factors known to be involved in self-renewal and cell proliferation. Indeed, these retroviruses were silenced in iPS cells indicating an efficient reprogramming. The obtained iPS cells were similar to human ESC (hESC) in respect to their morphology, proliferation, gene expression, *in vitro* differentiation and teratoma formation (Yu *et al.*, 2007). Therefore, iPS cells should resemble hESC differentiation and were used for microglial differentiation.

The differentiation protocol for human microglia from iPS cells was derived from the protocol for mouse ESdM differentiation developed in our laboratory (Napoli *et al.*, 2009). Since human iPS cells are different from mouse counterparts, the mouse protocol had to be adapted to the human system. Both mESC and iPS cells were cultivated on irradiated mouse embryonic fibroblasts. While mESC are dependent on leukaemia inhibitory factor (Matsuda *et al.*, 1999), the cultivation of iPS cells requires FGF2 for self-renewal (Amit *et al.*, 2000). In the study at hand, spontaneous differentiation of iPS cells to EBs was induced by removal of self-renewal signals coming from feeder cells and FGF2. EBs were plated after 8 days in culture. At this stage, EBs were positive for nestin as well as CD45 and Iba1, indicating the development of neuronal cells and macrophages/microglia. In the next step, neural differentiation was induced. Immunostaining revealed CD45 positive cells within a network of neuronal cells. These findings showed that the differentiation procedure led to a mixed culture of neuronal and microglial cells. The CD45 positive cells were isolated and enriched in medium supplemented with GM-CSF to enhance proliferation. In contrast to mouse ESdM, the obtained human microglial lines required a very long time interval up to 4 months for maturation of the microglial precursors from the mixed precursor cell population. Furthermore, a transient application of the growth factor GM-CSF was essential. After some days in culture in medium supplemented with GM-CSF, human microglial precursors started to proliferate and build processes. Staining for the microglial markers Iba1 and CD68 showed a pure population of microglial precursors (iPSdM). Upon isolation, iPSdM could be kept in culture for up to 25

passages without changing their morphology. The iPSdM showed an exponential growth rate with a mean doubling time of about 26 h.

4.1.2 Phenotype of iPSdM

Microglial cells share several markers with other immune cells like macrophages. However, myeloid cells can be distinguished from each other by a combination of phenotypic characterization, location and function (Ransohoff and Cardona, 2010). Therefore, iPSdM were investigated in regard to several marker expressions. Microglia are described as CD45 and CD11b positive (Guillemin and Brew, 2004). CD45 is a transmembrane protein with intrinsic tyrosine phosphatase activity. This protein is expressed on nucleated hematopoietic cells and is involved in cellular processes like linkage of immunoreceptor signaling with cytokine secretion and cell survival. CD11b belongs to the integrin family and together with CD18 forms the complement receptor 3 which is involved in phagocyte adhesion, migration and ingestion of complement-opsonized particles. Flow cytometry analysis confirmed the expression of both CD45 and CD11b on iPSdM hinting towards a microglial phenotype. Furthermore, iPSdM expressed CD11c (subunit of the complement receptor 4), CD16/32 (Fcγ receptor III and II), CD36 (scavenger receptor B) and the fractalkine receptor CX3CL1. The expression of the co-stimulatory molecules CD40 and CD86 (B7.2) as well as CD29 and CD49d (members of the integrin family) demonstrated their involvement in immunoregulatory functions. It is reported that microglia are able to present antigens via MHC class I and II. However, under non-activated conditions MHC class II expression is low (Peudenier *et al.*, 1991; Benveniste *et al.*, 2001). This is consistent with findings in iPSdM which express low levels of MHC class II under unstimulated conditions.

CD14 can act as associated co-receptor of the toll like receptor (TLR) 4 to enhance cell activation via LPS (Viriyakosol *et al.*, 2000). Unstimulated iPSdM did not or just slightly express CD14, while it could be upregulated after LPS and IFNγ stimulation. This result coincides with data found in primary human microglia where unstimulated microglia showed no expression of CD14 while mRNA levels of CD14 increased over time after LPS stimulation (Melief *et al.*, 2012).

Furthermore, iPSdM showed expression of CD206 (mannose receptor) which promotes phagocytosis and endocytosis and therefore is thought to be involved in innate immunity (Gordon, 2003). A recent publication showed that human primary

microglia, in contrast to macrophages, were negative for CD206 (Melief *et al.*, 2012). The difference to iPSdM might occur due to the different generation procedure. Primary human microglia were isolated using density gradient followed by magnetic-activated cell sorting. This procedure could lead to a pro-inflammatory activation of these cells. High expression of MHC class II protein, which is usually induced after activation, indicates that these cells are pro-inflammatory activated and therefore CD206 is downregulated.

The expression of Siglec-11 was observed on iPSdM. Siglecs are immuno-modulatory receptors which can be divided into two subgroups, the evolutionarily highly conserved Siglecs and the CD33-related Siglecs like Siglec-11, which are subject to rapid evolutionary changes (Crocker *et al.*, 2007). Siglecs are mainly expressed in the hematopoietic and immune system and can mediate cell-cell interactions. In the brain, Siglec-11 is exclusively expressed on microglia and might be involved in the regulation of innate immune responses (Angata *et al.*, 2002).

The iPSdM were generated from pluripotent stem cells, thus the expression of the hematopoietic stem cell marker CD34 was investigated. Indeed, CD34 was absent on iPSdM lines indicating that iPSdM were fully differentiated.

In summary, generated iPSdM lines showed a typical marker expression profile including CD11b, CD11c, CD16/32, CD45, CD68, CD86 and Iba1 as previously described for primary cells and microglia derived from neuropathological stainings (Ford *et al.*, 1995; Guillemin and Brew, 2004; Gibbons and Dragunow, 2010; Melief *et al.*, 2012).

4.1.3 Functionality of iPSdM

To further investigate the characteristics of iPSdM, different functional assays were performed.

One typical feature of microglia is the inducibility of pro-inflammatory cytokines (Hanisch, 2002). In the study at hand, LPS and IFNγ were used as exogenous or endogenous inflammatory triggers to induce TNFα and iNOS gene transcription. LPS is a component of the outer membrane of gram-negative bacteria and acts as an endotoxin activating the TLR4 whose signaling cascade leads to the production of pro-inflammatory cytokines (Viriyakosal *et al.*, 2000). IFNγ is secreted by $CD4^+$

T helper cell type I, $CD8^+$ cytotoxic lymphocytes and natural killer cells. It has antiviral, immunoregulatory and anti-tumor properties (Vila-del Sol *et al.*, 2008).

TNFα is a cytokine that stimulates the acute phase reaction and is involved in systemic inflammation. The main function of TNFα is the regulation of immune cells. Furthermore, TNFα is described to induce apoptotic cell death and inhibit tumorigenesis (Vujanovic, 2011; Montgomery and Bowers, 2012). Macrophages are the main producers of TNFα, but microglial activation by LPS or other bacterial products results in its production as well (Nakajima and Kohsaka, 1993; Smith *et al.*, 2012).

Real-time RT-PCR data of iPSdM showed the upregulation of TNFα transcript levels to 3.3 fold after 6 h of LPS stimulation. The inducibility of TNFα gene transcripts after LPS stimulation indicates that LPS acts as immunostimulatory substance for iPSdM. Data are in line with literature showing that LPS treatment of human fetal microglia led to increased TNFα levels after 2 to 8 h of stimulation, while the amount decreased within 24 to 48 h to the basic level (Lee *et al.*, 1993). On the other hand, IFNγ did not induce TNFα gene transcription in iPSdM after 6 h of stimulation. The induction of cytokine transcripts seems to be dependent on the time and type of stimulation. Studies on mouse macrophages showed the inducibility of TNFα by IFNγ up to 4 h of stimulation. After 16 h of IFNγ stimulation, TNFα levels decreased to their basic level (Vila-del Sol *et al.*, 2008). Using adult human microglia, another publication demonstrated increased TNFα transcription to about 2.5 fold by IFNγ after 8 h of stimulation (Becher *et al.*, 1996). Data of iPSdM showed that IFNγ stimulation had no impact on TNFα gene transcription within the first 6 h. Further experiments with different stimulation times would result in more information about the ability of iPSdM to react on IFNγ stimulation with increased TNFα transcription. As iPSdM are generated *in vitro*, the obtained microglial lines did not receive intrinsic or extrinsic factors, which might be a reason for different behavior in response to pro-inflammatory stimulation. For that reason iPSdM are defined as microglial precursor cells.

The enzyme iNOS can be induced by immunostimulatory cytokines, bacterial products and other substances (Aktan, 2004; Kleinert *et al.*, 2004). It is responsible for the synthesis of NO from arginine. NO is a free radical that can react with superoxide to form peroxynitrite thus leading to cell toxicity. Therefore, iNOS is involved in immune defence via antimicrobial and antitumoral activities.

However, there seemed to be species specific differences in the production of NO. While mouse and rat microglia produce high amounts of NO by activated iNOS, human microglial NO was almost undetectable (Colton *et al.*, 1996). Hence, iPSdM were investigated regarding their ability to induce iNOS gene transcription after stimulation. Real-time RT-PCR data of iPSdM showed no upregulation of iNOS after LPS or IFNγ stimulation. Furthermore, NO production was not increased after LPS and IFNγ stimulation (data not shown). It is unclear why human microglia do not produce NO in substantial amounts. But for human endothelial cells, it has been shown that iNOS is epigenetically silenced (Chan *et al.*, 2005).

Phagocytosis capacity, an important hallmark of microglia, is a highly coordinated process mainly regulated by environmental signals. Two main receptor types are involved in phagocytosis - the first, like TLRs, recognizes pathogens and the second, recognizes apoptotic material (Napoli and Neumann, 2009). Alzheimer's disease is characterized by extracellular amyloid β (Aβ) plaque formation. The aggregated form of Aβ is known to activate microglia through different receptors including TLRs (Landreth and Reed-Geaghan, 2009; Saijo and Glass, 2011). The clearance of Aβ-plaques might be due to microglia-mediated phagocytosis (Napoli *et al.*, 2009; Lee and Landreth, 2010).

Standard *in vitro* assays to investigate the phagocytosis capacity of microglia includes fibrillary Aβ and microsphere beads uptake. The assay system for the phagocytosis capacity of iPSdM in respect to Aβ determined that 18 % of unstimulated iPSdM were able to phagocytose Aβ. Stimulation with LPS or IFNγ significantly increased Aβ uptake by nearly 200 %. Thus, LPS and IFNγ act as stimulatory substance to increase Aβ phagocytosis.

In a second assay, iPSdM were incubated with fluorescent labeled microsphere beads and the number of positive cells was determined using flow cytometry. Cells were detached from the culture dish using trypsin to remove unspecific bound beads on the surface of the cells. Furthermore, only cells with fluorescent signals for more than one bead were taken into account. Unstimulated iPSdM showed an uptake of 33 % beads. LPS stimulation led to a slight, but not significant increase in beads phagocytosis to 40 %, whereas IFNγ stimulation had no impact.

The amount of microsphere beads phagocytosed by human iPSdM was comparable or even slightly higher compared to mouse ESdM (Beutner *et al.*, 2010). However, the used concentration and incubation time with beads between mouse and human stem cell-derived microglia differed. Since iPSdM were incubated with half the concentration of beads and for a shorter time period than ESdM, it appears that iPSdM are more potent in phagocytosis of microsphere beads. In contrast, phagocytosis of Aβ was reduced in iPSdM compared to both unstimulated mouse primary microglia and ESdM which showed an uptake of Aβ in the range of 30 to 60 % (Gaikwad *et al.*, 2009; Napoli *et al.*, 2009).
Differences between the mouse and human system could occur due to differently expressed proteins such as Siglecs. Some receptors of the Siglec family including Siglec-11 are exclusively expressed in humans without a counterpart in mice, while other CD33-related Siglecs show differences in the signaling cascade between mice and humans (Crocker *et al.*, 2007). Mouse CD33 can lead to an activatory signaling cascade whereas human CD33 exhibits, similar to Siglec-11, an inhibitory signaling (Brinkman-Van der Linden *et al.*, 2003; Varki, 2009; Wang and Neumann, 2010). Therefore, studies including the involvement of Siglecs are not comparable between mice and humans due to species differences and different signaling cascades. Genome-wide association studies demonstrated a high association of late-onset Alzheimer's disease in humans with polymorphisms in the CD33 gene (Hollingworth *et al.*, 2011; Naj *et al.*, 2011). Thus, iPSdM expressing inhibitory Siglecs (Siglec-11; CD33) might better reflect the situation of Alzheimer's disease, where Aβ is not properly cleared. Therefore, iPSdM might serve as a novel tool to study the recently described link between late onset Alzheimer's disease and CD33.

The chemokine CX3CL1 (fractalkine) is constitutively expressed by neurons and can promote chemotaxis (Re and Przedborski, 2006). Studies with transgenic mice encoding GFP under the promoter of the fractalkine receptor demonstrated that microglia are the only cell type in the CNS expressing the corresponding receptor CX3CR1 (Jung *et al.*, 2000). The signaling via CX3CL1-CX3CR1 seems to be important for the neuron-microglia interaction. CX3CR1 knockout mice demonstrated higher microglial activity and increased neuronal death in response to inflammatory and neurotoxic stimuli (Cardona *et al.*, 2006).

Primary mouse microglia were shown to migrate towards fractalkine (Napoli *et al.*, 2009). Flow cytometry data revealed the expression of CX3CR1 by iPSdM. Therefore, a migratory potential of iPSdM towards fractalkine could be expected. Using a transwell-system, the number of microglia which migrated towards fractalkine was analyzed. The evaluation showed that iPSdM display the capacity to migrate towards fractalkine. The number of migrated cells increased by approximately three-fold up to a concentration of 15 ng/ml fractalkine in comparison to undirected migration. Thus, iPSdM responded to fractalkine *in vitro* with migration in a dose-dependent manner.

Furthermore, the migration of iPSdM *in vivo* was analyzed. After intracerebral transplantation into immunodeficient mice, iPSdM also showed migration *in vivo*. Transplanted iPSdM developed typical microglial processes and integrated into the brain tissue. Since microglial cells might degenerate in the aging brain (Streit *et al.*, 2008) or in Alzheimer's disease (Streit *et al.*, 2009) and the natural source (yolk sac derived macrophages) is no longer available, iPSdM could form a novel source for a replacement therapy of senescent microglia.

4.2 iPSdM as a model for SOD1-mediated ALS

ALS is a late-onset neurodegenerative disease mainly affecting motor neurons in the brain and spinal cord (Bento-Abreu *et al.*, 2010). Mutations in the Cu/Zn SOD1 gene are the most common form of inherited ALS, accounting for 20 % of all familial ALS forms and corresponding to 1 – 2 % of all ALS cases (Boillee *et al.*, 2006a). A pathogenic role of microglia in ALS was suggested based on data of the SOD1 animal model over-expressing mutant human SOD1 G37R (Boillee *et al.*, 2006b). Conditional inactivation of mutated SOD1 in $CD11b^+$ microglia extended the survival of mice by preventing disease progression, particularly during the late phase of disease (Boillee *et al.*, 2006b). Active involvement of microglia in ALS was also shown in another study using PU.1-deficient mice which lack macrophages, neutrophils, B and T cells and microglia (Beers *et al.*, 2008). These mice were crossed to mice expressing the SOD1 G93A gene and then received bone marrow transplants from wildtype mice resulting in donor-derived microglia. Mice reconstituted with wildtype microglia showed significantly longer survival and decreased motor neuron loss, indicating a pathology-promoting role of

SOD1 G93A microglial cells. Thus, both approaches indicated that microglia are not involved in the onset but in the progression of the disease. However, the exact role of microglia in SOD1-mediated ALS is not fully understood.

Apparently, neuroinflammation contributes to motor neuron damage. Increased TNFα levels in the brain and spinal cord of mice coincide with the onset of motor neuron dysfunction (Strong, 2003). Furthermore, microglial contribution to neuronal impairment was demonstrated. The supernatant of LPS stimulated microglial cells induced motor neuron cell death through a TNFα-dependent pathway (He *et al.*, 2002).
Therefore, relative TNFα gene transcripts of iPSdM expressing GFP, wt or mutant SOD1 after stimulation with LPS, IFNγ or TNFα were investigated. Similar to non-transduced iPSdM, IFNγ stimulation did not increase TNFα transcript levels in any cell line. Additionally, TNFα stimulation neither had an effect in any cell line on TNFα transcription resembling data found in human fetal microglia where TNFα stimulation did not lead to TNFα cytokine production (Lee *et al.*, 1993). In contrast, LPS stimulation increased TNFα transcript levels in comparison to unstimulated cells in all cell lines. Contrary to literature, no significant difference in TNFα upregulation was observed between GFP or SOD1 wt and mutant SOD1 expressing iPSdM. But, experiments with adult mice ubiquitously expressing human SOD1 G93A demonstrated higher release of TNFα levels by SOD1 G93A-microglia in comparison to wt cells (Weydt *et al.*, 2004). However, this effect seemed to be age-dependent since SOD1 G93A and wt microglia from neonatal mice showed similar TNFα levels after LPS stimulation. Since iPSdM are generated based on embryonic differentiation, these cells might imitate more fetal or embryonic cell behavior. Thus, iPSdM might not reflect age-dependent effects of mSOD1 expressing microglia. With age, cells enter into growth arrest termed replicative senescence associated with telomere shortening and changes in gene expression profile (Chen *et al.*, 2007). It became evident that replicative senescence is an example for a more widespread response termed cellular senescence, which can be induced by substances that cause DNA damage, strong mitogenic signals or disrupt heterochromatin. As *in vitro* model for aging research, oxidative stress is used to induce cellular senescence for example by hydrogen peroxide. Thus, this method could provide the opportunity to study age-

dependent effects on the stimulation of TNFα transcription by mutant SOD1 expressing iPSdM.

So far, most knowledge on SOD1-mediated ALS is based on mouse models expressing mSOD1. Whether results obtained in mouse are comparable to the human system remains to be assessed. In contrast to rodent microglia, human microglia do not upregulate NO after pro-inflammatory stimulation (Peterson *et al.*, 1994). Such species difference has been claimed to be responsible for failure of translation of anti-inflammatory therapies from animal models to clinical therapy of patients suffering from neurodegenerative diseases (Dragunow, 2008). In addition, this diversity could lead to different results when comparing data from the mouse and the human system. Thus, iPSdM provide an essential tool to study the involvement of human microglia in neurodegenerative diseases.

Mitochondria represent the energy source of the cell being involved in cell respiratory processes, apoptosis and free radical production (Filosto *et al.*, 2011). Ultrastructural and functional alterations of mitochondria were detected in several neurodegenerative diseases such as Alzheimer's, Parkinson's, Huntington's disease and ALS (Filosto *et al.*, 2011). Furthermore, data indicate the involvement of mitochondrial damage in motor neuron degeneration in mice expressing mSOD1 (Wong *et al.*, 1995; Kong and Xu, 1998). Changes in the electron-transport chain (ETC) in mitochondria were shown in human spinal cord samples of patients with sporadic ALS (Fujita *et al.*, 1996; Borthwick *et al.*, 1999) and brain tissue of patients with SOD1-mediated ALS (Bowling *et al.*, 1993; Browne *et al.*, 1998). However, studies of mitochondrial alterations in ALS in microglia are absent.

In this work at hand, mSOD1 expressing iPSdM were investigated regarding their mitochondrial enzyme activities compared to SOD1 wt expressing cells. No differences were measured for complex I, IV and citrate synthase activities between wt and mSOD1 expressing iPSdM. Results obtained for complex IV are in line with data from spinal cord of rats expressing SOD1 G93A (Li *et al.*, 2010) and human brain tissue from familial ALS patients (Bowling *et al.*, 1993) showing no difference in complex IV activity. In contrast, outcome for complex I is different to publications showing affected activity in mSOD1 G93A rodent models (Browne *et al.*, 1998; Jung *et al.*, 2002; Li *et al.*, 2010) and human brain tissue from patients

with SOD1-mediated ALS (Bowling *et al.*, 1993). However, most studies investigated mitochondrial alterations in the whole tissue or concentrated on motor neurons alone regardless of other cell types like glial cells. Mitochondria are flexible organelles with structural diversity among tissue and species (Mannella, 2008). Investigations of mouse models for Parkinson's disease revealed different levels of ultrastructural damage in mitochondria of neurons and glial cells (Schmidt *et al.*, 2011). Therefore, a diverse vulnerability between neurons and microglia for mSOD1 on mitochondria could be likely.

Respiratory burst describes the release of ROS by phagocytes to degrade internalized particles and bacteria. The most important ROS are NO, superoxide and hydrogen peroxide (H_2O_2) which are toxic to microbial particles. Previous studies suggested a role of oxidative damage in the pathogenesis of ALS and a possible link to the expression of mSOD1. Overexpression of different mSOD1 in human neuroblastoma cell lines led to increased mitochondrial (Zimmerman *et al.*, 2007) and cytosolic (Beretta *et al.*, 2003) ROS production. Furthermore, increased superoxide levels were detected in the spinal cord and brain of SOD1 G93A expressing mice (Harraz *et al.*, 2008).

In the present study, superoxide production by mSOD1 expressing iPSdM was investigated in either unstimulated cells or cells stimulated with TNFα, LPS or IFNγ. Among the different cell lines nearly no difference in superoxide production was observed in unstimulated cells. But, superoxide production was increased after TNFα stimulation in iPSdM-SOD1 G37R in comparison to SOD1 wt cells, but no change was detected after LPS or IFNγ treatment. In contrast, iPSdM-SOD1 G85R showed no difference in superoxide production after any stimulation compared to SOD1 wt cells. Differences between the mutations could occur due to different dismutase activities of the mSOD1 proteins. Although all three are gain-of-function mutations, SOD1 G85R shows no difference in SOD1 activity whereas SOD1 G37R and SOD1 G93A have 3 – 14 fold increased activity levels (Gurney *et al.*, 1994; Wong *et al.*, 1995; Bruijn *et al.*, 1997). Furthermore, studies in mice expressing different mSOD1 suggest that SOD1 mutations seem to have specific effects on ALS pathogenesis. Knockdown of SOD1 G85R in astrocytes in $G85R^{flox}$ transgenic mice delayed disease onset and duration (Wang *et al.*, 2011), whereas loss of astrocytic SOD1 G37R affected only the late phase of the disease

(Yamanaka *et al.*, 2008). Different influences of the mutations in disease progression suggest diverse effects also in other mechanisms involved in ALS pathogenesis such as ROS production. The present study demonstrates an increase in superoxide production in iPSdM-SOD1 G93A after LPS or IFNγ but not TNFα stimulation compared to SOD1 wt cells. Data are in line with a previous publication showing increased superoxide and NO levels after LPS stimulation in SOD1 G93A mouse primary microglia in comparison to wt cells (Xiao *et al.*, 2007). The NADPH oxidase was suggested as main source of ROS production in microglia (Harraz *et al.*, 2008). It is a membrane-bound enzyme complex consisting of six subunits and responsible for the reduction of oxygen to superoxide (Babior, 2004). NOX2, a subunit of the NADPH oxidase, is regulated by the GTPase, Rac1. Under reducing conditions, SOD1 can bind to RAC1, thereby inhibiting its GTPase activity leading to NOX2 activation, followed by superoxide production and conversion into H_2O_2 by SOD1 (Harraz *et al.*, 2008). Increased H_2O_2 levels in turn lead to the dissociation of SOD1 from Rac1, inhibition of NOX2 and finally reduced superoxide and H_2O_2 production. However, this redox-sensitive uncoupling of SOD1 from Rac1 is defect in mSOD1 expressing microglia leading to increased superoxide levels in unstimulated cells (Harraz *et al.*, 2008). Whether the effect of increased superoxide production by iPSdM expressing SOD1 G37R or G93A after TNFα or LPS/IFNγ stimulation is mediated via the NADPH oxidase has to be determined. Treatment with apocynin, an inhibitor of the NADPH oxidase, or lentiviral knockdown of a subunit of the NADPH oxidase like NOX2 could give further insights into the mechanism behind.

To conclude, iPSdM present a novel tool for systems biology and might be suitable for drug development to understand and target the microglial pathways involved in human neuroinflammatory diseases.

5 References

Aktan F (2004) iNOS-mediated nitric oxide production and its regulation. Life Sci 75:639-653.

Alliot F, Godin I, Pessac B (1999) Microglia derive from progenitors, originating from the yolk sac, and which proliferate in the brain. Brain Res Dev Brain Res 117:145-152.

Amit M, Carpenter MK, Inokuma MS, Chiu CP, Harris CP, Waknitz MA, Itskovitz-Eldor J, Thomson JA (2000) Clonally derived human embryonic stem cell lines maintain pluripotency and proliferative potential for prolonged periods of culture. Dev Biol 227:271-278.

Andersen PM (2006) Amyotrophic lateral sclerosis associated with mutations in the CuZn superoxide dismutase gene. Curr Neurol Neurosci Rep 6:37-46.

Angata T, Kerr SC, Greaves DR, Varki NM, Crocker PR, Varki A (2002) Cloning and characterization of human Siglec-11. A recently evolved signaling molecule that can interact with SHP-1 and SHP-2 and is expressed by tissue macrophages, including brain microglia. J Biol Chem 277:24466-24474.

Babior BM (2004) NADPH oxidase. Curr Opin Immunol 16:42-47.

Becher B, Fedorowicz V, Antel JP (1996) Regulation of CD14 expression on human adult central nervous system-derived microglia. J Neurosci Res 45:375-381.

Beers DR, Henkel JS, Zhao W, Wang J, Appel SH (2008) CD4+ T cells support glial neuroprotection, slow disease progression, and modify glial morphology in an animal model of inherited ALS. Proc Natl Acad Sci U S A 105:15558-15563.

Bento-Abreu A, Van Damme P, Van Den Bosch L, Robberecht W (2010) The neurobiology of amyotrophic lateral sclerosis. Eur J Neurosci 31:2247-2265.

Benveniste EN, Nguyen VT, O'Keefe GM (2001) Immunological aspects of microglia: relevance to Alzheimer's disease. Neurochem Int 39:381-391.

Beretta S, Sala G, Mattavelli L, Ceresa C, Casciati A, Ferri A, Carri MT, Ferrarese C (2003) Mitochondrial dysfunction due to mutant copper/zinc superoxide dismutase associated with amyotrophic lateral sclerosis is reversed by N-acetylcysteine. Neurobiol Dis 13:213-221.

Bertrand JY, Jalil A, Klaine M, Jung S, Cumano A, Godin I (2005) Three pathways to mature macrophages in the early mouse yolk sac. Blood 106:3004-3011.

Beutner C, Roy K, Linnartz B, Napoli I, Neumann H (2010) Generation of microglial cells from mouse embryonic stem cells. Nat Protoc 5:1481-1494.

Biber K, Neumann H, Inoue K, Boddeke HW (2007) Neuronal 'On' and 'Off' signals control microglia. Trends Neurosci 30:596-602.

Blasi E, Barluzzi R, Bocchini V, Mazzolla R, Bistoni F (1990) Immortalization of murine microglial cells by a v-raf/v-myc carrying retrovirus. J Neuroimmunol 27:229-237.

Block ML, Hong JS (2005) Microglia and inflammation-mediated neurodegeneration: multiple triggers with a common mechanism. Prog Neurobiol 76:77-98.

Block ML, Zecca L, Hong JS (2007) Microglia-mediated neurotoxicity: uncovering the molecular mechanisms. Nat Rev Neurosci 8:57-69.

Bocchini V, Mazzolla R, Barluzzi R, Blasi E, Sick P, Kettenmann H (1992) An immortalized cell line expresses properties of activated microglial cells. J Neurosci Res 31:616-621.

Boillee S, Vande Velde C, Cleveland DW (2006a) ALS: a disease of motor neurons and their nonneuronal neighbors. Neuron 52:39-59.

Boillee S, Yamanaka K, Lobsiger CS, Copeland NG, Jenkins NA, Kassiotis G, Kollias G, Cleveland DW (2006b) Onset and progression in inherited ALS determined by motor neurons and microglia. Science 312:1389-1392.

Borthwick GM, Johnson MA, Ince PG, Shaw PJ, Turnbull DM (1999) Mitochondrial enzyme activity in amyotrophic lateral sclerosis: implications for the role of mitochondria in neuronal cell death. Ann Neurol 46:787-790.

Bowling AC, Schulz JB, Brown RH, Jr., Beal MF (1993) Superoxide dismutase activity, oxidative damage, and mitochondrial energy metabolism in familial and sporadic amyotrophic lateral sclerosis. J Neurochem 61:2322-2325.

Brinkman-Van der Linden EC, Angata T, Reynolds SA, Powell LD, Hedrick SM, Varki A (2003) CD33/Siglec-3 binding specificity, expression pattern, and consequences of gene deletion in mice. Mol Cell Biol 23:4199-4206.

Browne SE, Bowling AC, Baik MJ, Gurney M, Brown RH, Jr., Beal MF (1998) Metabolic dysfunction in familial, but not sporadic, amyotrophic lateral sclerosis. J Neurochem 71:281-287.

Bruijn LI, Houseweart MK, Kato S, Anderson KL, Anderson SD, Ohama E, Reaume AG, Scott RW, Cleveland DW (1998) Aggregation and motor neuron toxicity of an ALS-linked SOD1 mutant independent from wild-type SOD1. Science 281:1851-1854.

Bruijn LI, Becher MW, Lee MK, Anderson KL, Jenkins NA, Copeland NG, Sisodia SS, Rothstein JD, Borchelt DR, Price DL, Cleveland DW (1997) ALS-linked SOD1 mutant G85R mediates damage to astrocytes and promotes rapidly progressive disease with SOD1-containing inclusions. Neuron 18:327-338.

Cao X, Shores EW, Hu-Li J, Anver MR, Kelsall BL, Russell SM, Drago J, Noguchi M, Grinberg A, Bloom ET, et al. (1995) Defective lymphoid development in mice lacking expression of the common cytokine receptor gamma chain. Immunity 2:223-238.

Cardona AE, Pioro EP, Sasse ME, Kostenko V, Cardona SM, Dijkstra IM, Huang D, Kidd G, Dombrowski S, Dutta R, Lee JC, Cook DN, Jung S, Lira SA, Littman DR, Ransohoff RM (2006) Control of microglial neurotoxicity by the fractalkine receptor. Nat Neurosci 9:917-924.

Cartier L, Hartley O, Dubois-Dauphin M, Krause KH (2005) Chemokine receptors in the central nervous system: role in brain inflammation and neurodegenerative diseases. Brain Res Brain Res Rev 48:16-42.

Chan GC, Fish JE, Mawji IA, Leung DD, Rachlis AC, Marsden PA (2005) Epigenetic basis for the transcriptional hyporesponsiveness of the human inducible nitric oxide synthase gene in vascular endothelial cells. J Immunol 175:3846-3861.

Chan WY, Kohsaka S, Rezaie P (2007) The origin and cell lineage of microglia: new concepts. Brain Res Rev 53:344-354.

Chen JH, Ozanne SE, Hales CN (2007) Methods of cellular senescence induction using oxidative stress. Methods Mol Biol 371:179-189.

Colton C, Wilt S, Gilbert D, Chernyshev O, Snell J, Dubois-Dalcq M (1996) Species differences in the generation of reactive oxygen species by microglia. Mol Chem Neuropathol 28:15-20.

Crocker PR, Paulson JC, Varki A (2007) Siglecs and their roles in the immune system. Nat Rev Immunol 7:255-266.

del Rio-Hortega P (1933) Art and artifice in the science of histology. Histopathology 22:515-525.

Dimos JT, Rodolfa KT, Niakan KK, Weisenthal LM, Mitsumoto H, Chung W, Croft GF, Saphier G, Leibel R, Goland R, Wichterle H, Henderson CE, Eggan K (2008) Induced pluripotent stem cells generated from patients with ALS can be differentiated into motor neurons. Science 321:1218-1221.

Dragunow M (2008) The adult human brain in preclinical drug development. Nat Rev Drug Discov 7:659-666.

Engelhardt JI, Appel SH (1990) IgG reactivity in the spinal cord and motor cortex in amyotrophic lateral sclerosis. Arch Neurol 47:1210-1216.

Filosto M, Scarpelli M, Cotelli MS, Vielmi V, Todeschini A, Gregorelli V, Tonin P, Tomelleri G, Padovani A (2011) The role of mitochondria in neurodegenerative diseases. J Neurol 258:1763-1774.

Ford AL, Goodsall AL, Hickey WF, Sedgwick JD (1995) Normal adult ramified microglia separated from other central nervous system macrophages by flow cytometric sorting. Phenotypic differences defined and direct ex vivo antigen presentation to myelin basic protein-reactive CD4+ T cells compared. J Immunol 154:4309-4321.

Fujita K, Yamauchi M, Shibayama K, Ando M, Honda M, Nagata Y (1996) Decreased cytochrome c oxidase activity but unchanged superoxide dismutase and glutathione peroxidase activities in the spinal cords of patients with amyotrophic lateral sclerosis. J Neurosci Res 45:276-281.

Furukawa Y, Torres AS, O'Halloran TV (2004) Oxygen-induced maturation of SOD1: a key role for disulfide formation by the copper chaperone CCS. Embo J 23:2872-2881.

Furukawa Y, Fu R, Deng HX, Siddique T, O'Halloran TV (2006) Disulfide cross-linked protein represents a significant fraction of ALS-associated Cu, Zn-superoxide dismutase aggregates in spinal cords of model mice. Proc Natl Acad Sci U S A 103:7148-7153.

Gaikwad S, Larionov S, Wang Y, Dannenberg H, Matozaki T, Monsonego A, Thal DR, Neumann H (2009) Signal regulatory protein-beta1: a microglial modulator of phagocytosis in Alzheimer's disease. Am J Pathol 175:2528-2539.

Garden GA, Moller T (2006) Microglia biology in health and disease. J Neuroimmune Pharmacol 1:127-137.

Gibbons HM, Dragunow M (2010) Adult human brain cell culture for neuroscience research. Int J Biochem Cell Biol 42:844-856.

Ginhoux F, Greter M, Leboeuf M, Nandi S, See P, Gokhan S, Mehler MF, Conway SJ, Ng LG, Stanley ER, Samokhvalov IM, Merad M (2010) Fate mapping analysis reveals that adult microglia derive from primitive macrophages. Science 330:841-845.

Giulian D, Baker TJ (1986) Characterization of ameboid microglia isolated from developing mammalian brain. J Neurosci 6:2163-2178.

Glass CK, Saijo K, Winner B, Marchetto MC, Gage FH (2010) Mechanisms underlying inflammation in neurodegeneration. Cell 140:918-934.

Gong YH, Parsadanian AS, Andreeva A, Snider WD, Elliott JL (2000) Restricted expression of G86R Cu/Zn superoxide dismutase in astrocytes results in astrocytosis but does not cause motoneuron degeneration. J Neurosci 20:660-665.

Gordon S (2003) Alternative activation of macrophages. Nat Rev Immunol 3:23-35.

Guillemin GJ, Brew BJ (2004) Microglia, macrophages, perivascular macrophages, and pericytes: a review of function and identification. J Leukoc Biol 75:388-397.

Gurney ME, Pu H, Chiu AY, Dal Canto MC, Polchow CY, Alexander DD, Caliendo J, Hentati A, Kwon YW, Deng HX, et al. (1994) Motor neuron degeneration in mice that express a human Cu,Zn superoxide dismutase mutation. Science 264:1772-1775.

Hall ED, Oostveen JA, Gurney ME (1998) Relationship of microglial and astrocytic activation to disease onset and progression in a transgenic model of familial ALS. Glia 23:249-256.

Hanisch UK (2002) Microglia as a source and target of cytokines. Glia 40:140-155.

Harraz MM, Marden JJ, Zhou W, Zhang Y, Williams A, Sharov VS, Nelson K, Luo M, Paulson H, Schoneich C, Engelhardt JF (2008) SOD1 mutations disrupt redox-sensitive Rac regulation of NADPH oxidase in a familial ALS model. J Clin Invest 118:659-670.

He BP, Wen W, Strong MJ (2002) Activated microglia (BV-2) facilitation of TNF-alpha-mediated motor neuron death in vitro. J Neuroimmunol 128:31-38.

Henkel JS, Beers DR, Siklos L, Appel SH (2006) The chemokine MCP-1 and the dendritic and myeloid cells it attracts are increased in the mSOD1 mouse model of ALS. Mol Cell Neurosci 31:427-437.

Henkel JS, Engelhardt JI, Siklos L, Simpson EP, Kim SH, Pan T, Goodman JC, Siddique T, Beers DR, Appel SH (2004) Presence of dendritic cells, MCP-1, and activated microglia/macrophages in amyotrophic lateral sclerosis spinal cord tissue. Ann Neurol 55:221-235.

Hollingworth P, Harold D, Sims R, Gerrish A, Lambert JC, Carrasquillo MM, Abraham R, Hamshere ML, Pahwa JS, Moskvina V, Dowzell K, Jones N, Stretton A, Thomas C, Richards A, Ivanov D, Widdowson C, Chapman J, Lovestone S, Powell J, Proitsi P, Lupton MK, Brayne C, Rubinsztein DC, Gill M, Lawlor B, Lynch A, Brown KS, Passmore PA, Craig D, McGuinness B, Todd S, Holmes C, Mann D, Smith AD, Beaumont H, Warden D, Wilcock G, Love S, Kehoe PG, Hooper NM, Vardy ER, Hardy J, Mead S, Fox NC, Rossor M, Collinge J, Maier W, Jessen F, Ruther E, Schurmann B, Heun R, Kolsch H, van den Bussche H, Heuser I, Kornhuber J, Wiltfang J, Dichgans M, Frolich L, Hampel H, Gallacher J, Hull M, Rujescu D, Giegling I, Goate AM, Kauwe JS, Cruchaga C, Nowotny P, Morris JC, Mayo K, Sleegers K, Bettens K, Engelborghs S, De Deyn PP, Van Broeckhoven C, Livingston G, Bass NJ, Gurling H, McQuillin A, Gwilliam R, Deloukas P, Al-Chalabi A, Shaw CE, Tsolaki M, Singleton AB, Guerreiro R, Muhleisen TW, Nothen MM, Moebus S, Jockel KH, Klopp N, Wichmann HE, Pankratz VS, Sando SB, Aasly JO, Barcikowska M, Wszolek ZK, Dickson DW, Graff-Radford NR, Petersen RC, et al. (2011) Common variants at ABCA7, MS4A6A/MS4A4E, EPHA1, CD33 and CD2AP are associated with Alzheimer's disease. Nat Genet 43:429-435.

Horvath RJ, Nutile-McMenemy N, Alkaitis MS, Deleo JA (2008) Differential migration, LPS-induced cytokine, chemokine, and NO expression in immortalized BV-2 and HAPI cell lines and primary microglial cultures. J Neurochem 107:557-569.

Inamdar M, Koch T, Rapoport R, Dixon JT, Probolus JA, Cram E, Bautch VL (1997) Yolk sac-derived murine macrophage cell line has a counterpart during ES cell differentiation. Dev Dyn 210:487-497.

Jaarsma D, Rognoni F, van Duijn W, Verspaget HW, Haasdijk ED, Holstege JC (2001) CuZn superoxide dismutase (SOD1) accumulates in vacuolated mitochondria in transgenic mice expressing amyotrophic lateral sclerosis-linked SOD1 mutations. Acta Neuropathol 102:293-305.

Janabi N, Peudenier S, Heron B, Ng KH, Tardieu M (1995) Establishment of human microglial cell lines after transfection of primary cultures of embryonic microglial cells with the SV40 large T antigen. Neurosci Lett 195:105-108.

Jung C, Higgins CM, Xu Z (2002) Mitochondrial electron transport chain complex dysfunction in a transgenic mouse model for amyotrophic lateral sclerosis. J Neurochem 83:535-545.

Jung S, Aliberti J, Graemmel P, Sunshine MJ, Kreutzberg GW, Sher A, Littman DR (2000) Analysis of fractalkine receptor CX(3)CR1 function by targeted deletion and green fluorescent protein reporter gene insertion. Mol Cell Biol 20:4106-4114.

Kang L, Wang J, Zhang Y, Kou Z, Gao S (2009) iPS cells can support full-term development of tetraploid blastocyst-complemented embryos. Cell Stem Cell 5:135-138.

Kaur C, Hao AJ, Wu CH, Ling EA (2001) Origin of microglia. Microsc Res Tech 54:2-9.

Keller G, Kennedy M, Papayannopoulou T, Wiles MV (1993) Hematopoietic commitment during embryonic stem cell differentiation in culture. Mol Cell Biol 13:473-486.

Kettenmann H, Hanisch UK, Noda M, Verkhratsky A (2011) Physiology of microglia. Physiol Rev 91:461-553.

Kleinert H, Pautz A, Linker K, Schwarz PM (2004) Regulation of the expression of inducible nitric oxide synthase. Eur J Pharmacol 500:255-266.

Kong J, Xu Z (1998) Massive mitochondrial degeneration in motor neurons triggers the onset of amyotrophic lateral sclerosis in mice expressing a mutant SOD1. J Neurosci 18:3241-3250.

Kreutzberg GW (1996) Microglia: a sensor for pathological events in the CNS. Trends Neurosci 19:312-318.

Landreth GE, Reed-Geaghan EG (2009) Toll-like receptors in Alzheimer's disease. Curr Top Microbiol Immunol 336:137-153.

Lee CY, Landreth GE (2010) The role of microglia in amyloid clearance from the AD brain. J Neural Transm 117:949-960.

Lee SC, Liu W, Dickson DW, Brosnan CF, Berman JW (1993) Cytokine production by human fetal microglia and astrocytes. Differential induction by lipopolysaccharide and IL-1 beta. J Immunol 150:2659-2667.

Li Q, Vande Velde C, Israelson A, Xie J, Bailey AO, Dong MQ, Chun SJ, Roy T, Winer L, Yates JR, Capaldi RA, Cleveland DW, Miller TM (2010) ALS-linked mutant superoxide dismutase 1 (SOD1) alters mitochondrial protein composition and decreases protein import. Proc Natl Acad Sci U S A 107:21146-21151.

Liao B, Zhao W, Beers DR, Henkel JS, Appel SH (2012) Transformation from a neuroprotective to a neurotoxic microglial phenotype in a mouse model of ALS. Exp Neurol 237:147-152.

Lino MM, Schneider C, Caroni P (2002) Accumulation of SOD1 mutants in postnatal motoneurons does not cause motoneuron pathology or motoneuron disease. J Neurosci 22:4825-4832.

Liu J, Lillo C, Jonsson PA, Vande Velde C, Ward CM, Miller TM, Subramaniam JR, Rothstein JD, Marklund S, Andersen PM, Brannstrom T, Gredal O, Wong PC, Williams DS, Cleveland DW (2004) Toxicity of familial ALS-linked SOD1 mutants from selective recruitment to spinal mitochondria. Neuron 43:5-17.

Mannella CA (2008) Structural diversity of mitochondria: functional implications. Ann N Y Acad Sci 1147:171-179.

Matsuda T, Nakamura T, Nakao K, Arai T, Katsuki M, Heike T, Yokota T (1999) STAT3 activation is sufficient to maintain an undifferentiated state of mouse embryonic stem cells. Embo J 18:4261-4269.

Melief J, Koning N, Schuurman KG, Van De Garde MD, Smolders J, Hoek RM, Van Eijk M, Hamann J, Huitinga I (2012) Phenotyping primary human microglia: Tight regulation of LPS responsiveness. Glia.

Montgomery SL, Bowers WJ (2012) Tumor necrosis factor-alpha and the roles it plays in homeostatic and degenerative processes within the central nervous system. J Neuroimmune Pharmacol 7:42-59.

Nagai A, Nakagawa E, Hatori K, Choi HB, McLarnon JG, Lee MA, Kim SU (2001) Generation and characterization of immortalized human microglial cell lines: expression of cytokines and chemokines. Neurobiol Dis 8:1057-1068.

Nagai A, Mishima S, Ishida Y, Ishikura H, Harada T, Kobayashi S, Kim SU (2005) Immortalized human microglial cell line: phenotypic expression. J Neurosci Res 81:342-348.

Naj AC, Jun G, Beecham GW, Wang LS, Vardarajan BN, Buros J, Gallins PJ, Buxbaum JD, Jarvik GP, Crane PK, Larson EB, Bird TD, Boeve BF, Graff-Radford NR, De Jager PL, Evans D, Schneider JA, Carrasquillo MM, Ertekin-Taner N, Younkin SG, Cruchaga C, Kauwe JS, Nowotny P, Kramer P, Hardy J, Huentelman MJ, Myers AJ, Barmada MM, Demirci FY, Baldwin CT, Green RC, Rogaeva E, St George-Hyslop P, Arnold SE, Barber R, Beach T, Bigio EH, Bowen JD, Boxer A, Burke JR, Cairns NJ, Carlson CS, Carney RM, Carroll SL, Chui HC, Clark DG, Corneveaux J, Cotman CW, Cummings JL, DeCarli C, DeKosky ST, Diaz-Arrastia R, Dick M, Dickson DW, Ellis WG, Faber KM, Fallon KB, Farlow MR, Ferris S, Frosch MP, Galasko DR, Ganguli M, Gearing M, Geschwind DH, Ghetti B, Gilbert JR, Gilman S, Giordani B, Glass JD, Growdon JH, Hamilton RL, Harrell LE, Head E, Honig LS, Hulette CM, Hyman BT, Jicha GA, Jin LW, Johnson N, Karlawish J, Karydas A, Kaye JA, Kim R, Koo EH, Kowall NW, Lah JJ, Levey AI, Lieberman AP, Lopez OL, Mack WJ, Marson DC, Martiniuk F, Mash DC, Masliah E, McCormick WC, McCurry SM, McDavid AN, McKee AC, Mesulam M, Miller BL, et al. (2011) Common variants at MS4A4/MS4A6E, CD2AP, CD33 and EPHA1 are associated with late-onset Alzheimer's disease. Nat Genet 43:436-441.

Nakajima K, Kohsaka S (1993) Functional roles of microglia in the brain. Neurosci Res 17:187-203.

Napoli I, Neumann H (2009) Microglial clearance function in health and disease. Neuroscience 158:1030-1038.

Napoli I, Kierdorf K, Neumann H (2009) Microglial precursors derived from mouse embryonic stem cells. Glia 57:1660-1671.

Nimmerjahn A, Kirchhoff F, Helmchen F (2005) Resting microglial cells are highly dynamic surveillants of brain parenchyma in vivo. Science 308:1314-1318.

Olah M, Raj D, Brouwer N, De Haas AH, Eggen BJ, Den Dunnen WF, Biber KP, Boddeke HW (2012) An optimized protocol for the acute isolation of human microglia from autopsy brain samples. Glia 60:96-111.

Park IH, Arora N, Huo H, Maherali N, Ahfeldt T, Shimamura A, Lensch MW, Cowan C, Hochedlinger K, Daley GQ (2008) Disease-specific induced pluripotent stem cells. Cell 134:877-886.

Peterson PK, Hu S, Anderson WR, Chao CC (1994) Nitric oxide production and neurotoxicity mediated by activated microglia from human versus mouse brain. J Infect Dis 170:457-460.

Peudenier S, Hery C, Montagnier L, Tardieu M (1991) Human microglial cells: characterization in cerebral tissue and in primary culture, and study of their susceptibility to HIV-1 infection. Ann Neurol 29:152-161.

Pramatarova A, Laganiere J, Roussel J, Brisebois K, Rouleau GA (2001) Neuron-specific expression of mutant superoxide dismutase 1 in transgenic mice does not lead to motor impairment. J Neurosci 21:3369-3374.

Prinz M, Priller J, Sisodia SS, Ransohoff RM (2011) Heterogeneity of CNS myeloid cells and their roles in neurodegeneration. Nat Neurosci 14:1227-1235.

Ransohoff RM, Perry VH (2009) Microglial physiology: unique stimuli, specialized responses. Annu Rev Immunol 27:119-145.

Ransohoff RM, Cardona AE (2010) The myeloid cells of the central nervous system parenchyma. Nature 468:253-262.

Ravichandran KS (2003) "Recruitment signals" from apoptotic cells: invitation to a quiet meal. Cell 113:817-820.

Re DB, Przedborski S (2006) Fractalkine: moving from chemotaxis to neuroprotection. Nat Neurosci 9:859-861.

Reaume AG, Elliott JL, Hoffman EK, Kowall NW, Ferrante RJ, Siwek DF, Wilcox HM, Flood DG, Beal MF, Brown RH, Jr., Scott RW, Snider WD (1996) Motor neurons in Cu/Zn superoxide dismutase-deficient mice develop normally but exhibit enhanced cell death after axonal injury. Nat Genet 13:43-47.

Rezaie P, Male D (2002) Mesoglia & microglia--a historical review of the concept of mononuclear phagocytes within the central nervous system. J Hist Neurosci 11:325-374.

Rock RB, Gekker G, Hu S, Sheng WS, Cheeran M, Lokensgard JR, Peterson PK (2004) Role of microglia in central nervous system infections. Clin Microbiol Rev 17:942-964, table of contents.

Rosen DR, Siddique T, Patterson D, Figlewicz DA, Sapp P, Hentati A, Donaldson D, Goto J, O'Regan JP, Deng HX, et al. (1993) Mutations in Cu/Zn superoxide dismutase gene are associated with familial amyotrophic lateral sclerosis. Nature 362:59-62.

Rowland LP, Shneider NA (2001) Amyotrophic lateral sclerosis. N Engl J Med 344:1688-1700.

Saijo K, Glass CK (2011) Microglial cell origin and phenotypes in health and disease. Nat Rev Immunol 11:775-787.

Schmidt S, Linnartz B, Mendritzki S, Sczepan T, Lubbert M, Stichel CC, Lubbert H (2011) Genetic mouse models for Parkinson's disease display severe pathology in glial cell mitochondria. Hum Mol Genet 20:1197-1211.

Smith JA, Das A, Ray SK, Banik NL (2012) Role of pro-inflammatory cytokines released from microglia in neurodegenerative diseases. Brain Res Bull 87:10-20.

Soldner F, Hockemeyer D, Beard C, Gao Q, Bell GW, Cook EG, Hargus G, Blak A, Cooper O, Mitalipova M, Isacson O, Jaenisch R (2009) Parkinson's disease patient-derived induced pluripotent stem cells free of viral reprogramming factors. Cell 136:964-977.

Soulet D, Rivest S (2008) Microglia. Curr Biol 18:R506-508.

Streit WJ (2002) Microglia as neuroprotective, immunocompetent cells of the CNS. Glia 40:133-139.

Streit WJ, Miller KR, Lopes KO, Njie E (2008) Microglial degeneration in the aging brain--bad news for neurons? Front Biosci 13:3423-3438.

Streit WJ, Braak H, Xue QS, Bechmann I (2009) Dystrophic (senescent) rather than activated microglial cells are associated with tau pathology and likely precede neurodegeneration in Alzheimer's disease. Acta Neuropathol 118:475-485.

Strong MJ (2003) The basic aspects of therapeutics in amyotrophic lateral sclerosis. Pharmacol Ther 98:379-414.

Subramaniam JR, Lyons WE, Liu J, Bartnikas TB, Rothstein J, Price DL, Cleveland DW, Gitlin JD, Wong PC (2002) Mutant SOD1 causes motor neuron disease independent of copper chaperone-mediated copper loading. Nat Neurosci 5:301-307.

Takahashi K, Yamanaka S (2006) Induction of pluripotent stem cells from mouse embryonic and adult fibroblast cultures by defined factors. Cell 126:663-676.

Takahashi K, Tanabe K, Ohnuki M, Narita M, Ichisaka T, Tomoda K, Yamanaka S (2007) Induction of pluripotent stem cells from adult human fibroblasts by defined factors. Cell 131:861-872.

Takashima Y, Era T, Nakao K, Kondo S, Kasuga M, Smith AG, Nishikawa S (2007) Neuroepithelial cells supply an initial transient wave of MSC differentiation. Cell 129:1377-1388.

Thomson JA, Itskovitz-Eldor J, Shapiro SS, Waknitz MA, Swiergiel JJ, Marshall VS, Jones JM (1998) Embryonic stem cell lines derived from human blastocysts. Science 282:1145-1147.

Tsan MF, Gao B (2004) Endogenous ligands of Toll-like receptors. J Leukoc Biol 76:514-519.

Varki A (2009) Natural ligands for CD33-related Siglecs? Glycobiology 19:810-812.

Vila-del Sol V, Punzon C, Fresno M (2008) IFN-gamma-induced TNF-alpha expression is regulated by interferon regulatory factors 1 and 8 in mouse macrophages. J Immunol 181:4461-4470.

Viriyakosol S, Mathison JC, Tobias PS, Kirkland TN (2000) Structure-function analysis of CD14 as a soluble receptor for lipopolysaccharide. J Biol Chem 275:3144-3149.

Vujanovic NL (2011) Role of TNF superfamily ligands in innate immunity. Immunol Res 50:159-174.

Wang L, Gutmann DH, Roos RP (2011) Astrocyte loss of mutant SOD1 delays ALS disease onset and progression in G85R transgenic mice. Hum Mol Genet 20:286-293.

Wang Y, Neumann H (2010) Alleviation of neurotoxicity by microglial human Siglec-11. J Neurosci 30:3482-3488.

Watanabe M, Dykes-Hoberg M, Culotta VC, Price DL, Wong PC, Rothstein JD (2001) Histological evidence of protein aggregation in mutant SOD1 transgenic mice and in amyotrophic lateral sclerosis neural tissues. Neurobiol Dis 8:933-941.

Weydt P, Yuen EC, Ransom BR, Moller T (2004) Increased cytotoxic potential of microglia from ALS-transgenic mice. Glia 48:179-182.

Wiedemann FR, Vielhaber S, Schroder R, Elger CE, Kunz WS (2000) Evaluation of methods for the determination of mitochondrial respiratory chain enzyme activities in human skeletal muscle samples. Anal Biochem 279:55-60.

Wong PC, Pardo CA, Borchelt DR, Lee MK, Copeland NG, Jenkins NA, Sisodia SS, Cleveland DW, Price DL (1995) An adverse property of a familial ALS-linked SOD1 mutation causes motor neuron disease characterized by vacuolar degeneration of mitochondria. Neuron 14:1105-1116.

Worms PM (2001) The epidemiology of motor neuron diseases: a review of recent studies. J Neurol Sci 191:3-9.

Xiao Q, Zhao W, Beers DR, Yen AA, Xie W, Henkel JS, Appel SH (2007) Mutant SOD1(G93A) microglia are more neurotoxic relative to wild-type microglia. J Neurochem 102:2008-2019.

Xu C, Inokuma MS, Denham J, Golds K, Kundu P, Gold JD, Carpenter MK (2001) Feeder-free growth of undifferentiated human embryonic stem cells. Nat Biotechnol 19:971-974.

Yamanaka K, Chun SJ, Boillee S, Fujimori-Tonou N, Yamashita H, Gutmann DH, Takahashi R, Misawa H, Cleveland DW (2008) Astrocytes as determinants of disease progression in inherited amyotrophic lateral sclerosis. Nat Neurosci 11:251-253.

Yu J, Vodyanik MA, Smuga-Otto K, Antosiewicz-Bourget J, Frane JL, Tian S, Nie J, Jonsdottir GA, Ruotti V, Stewart R, Slukvin, II, Thomson JA (2007) Induced pluripotent stem cell lines derived from human somatic cells. Science 318:1917-1920.

Zambidis ET, Peault B, Park TS, Bunz F, Civin CI (2005) Hematopoietic differentiation of human embryonic stem cells progresses through sequential hematoendothelial, primitive, and definitive stages resembling human yolk sac development. Blood 106:860-870.

Zhao W, Xie W, Le W, Beers DR, He Y, Henkel JS, Simpson EP, Yen AA, Xiao Q, Appel SH (2004) Activated microglia initiate motor neuron injury by a nitric oxide and glutamate-mediated mechanism. J Neuropathol Exp Neurol 63:964-977.

Zhao XY, Li W, Lv Z, Liu L, Tong M, Hai T, Hao J, Guo CL, Ma QW, Wang L, Zeng F, Zhou Q (2009) iPS cells produce viable mice through tetraploid complementation. Nature 461:86-90.

Zhou Y, Wang Y, Kovacs M, Jin J, Zhang J (2005) Microglial activation induced by neurodegeneration: a proteomic analysis. Mol Cell Proteomics 4:1471-1479.

Zimmerman MC, Oberley LW, Flanagan SW (2007) Mutant SOD1-induced neuronal toxicity is mediated by increased mitochondrial superoxide levels. J Neurochem 102:609-618.

IV Acknowledgements

I would like to thank Prof. Dr. Harald Neumann for giving me the opportunity to work with such an interesting topic, for supervision and support. I also thank Prof. Dr. Joachim Schultze for being my second supervisor. I thank Prof. Dr. Oliver Brüstle for creating a nice working atmosphere.

Special thank goes to Anke Leinhaas for helping me with mouse handling and stereotactic injection. I also would like to thank our collaborators Prof. Oliver Brüstle and Prof. Dr. Wolfram Kunz from the University of Bonn and Dr. Albrecht Clement from the University of Mainz.

Many thanks also go to my lab members who became friends and made work so much more fun. Thank you for your support, help and discussions.

Special thanks go to my friends and family, for all their support, help and understanding. Last but not least, I am deeply grateful for Stefan with all his love, encouragement, understanding and care.

V Erklärung/Declaration

I, Kristin Roy, hereby confirm that this work submitted is my own. This thesis has been written independently and with no other sources and aids than stated.
The presented thesis has not been submitted to another university and I have not applied for a doctorate procedure so far.

Hiermit versichere ich, dass die vorgelegte Arbeit – abgesehen von den ausdrücklich bezeichneten Hilfsmitteln – persönlich, selbständig und ohne Benutzung anderer als der angegebenen Hilfsmittel angefertigt wurde. Aus anderen Quellen direkt oder indirekt übernommene Daten und Konzepte sind unter Angabe der Quelle kenntlich gemacht worden.
Die vorliegende Arbeit wurde an keiner anderen Hochschule als Dissertation eingereicht. Ich habe früher noch keinen Promotionsversuch unternommen.

Bonn, August 2012

Kristin Roy